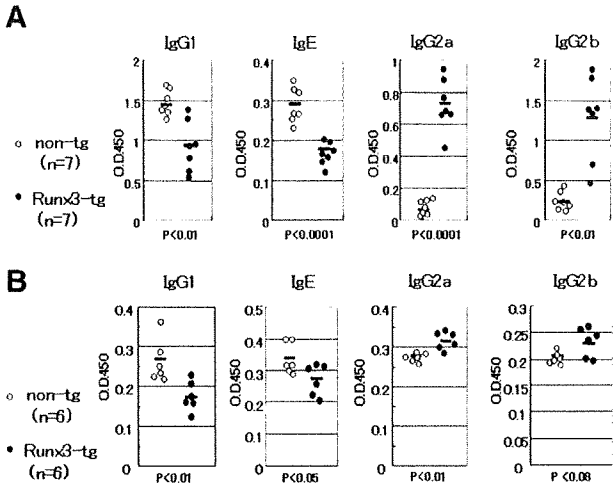

FIGURE 8. Ig titers in the sera of immunized *Runx3*-transgenic (tg) mice. Nontransgenic (non-tg) and *Runx3*-transgenic mice were injected s.c. or i.p. with OVA mixed with CFA (*A*) or aluminum hydroxide (*B*), respectively. After the second boosting injection, sera were collected, and the titers of IgG1, IgE, IgG2a, and IgG2b were measured by ELISA. Horizontal lines represent the average OD_{450} for each group. A statistically significant difference was detected between nontransgenic and *Runx3*-transgenic mice (*p* values are indicated).

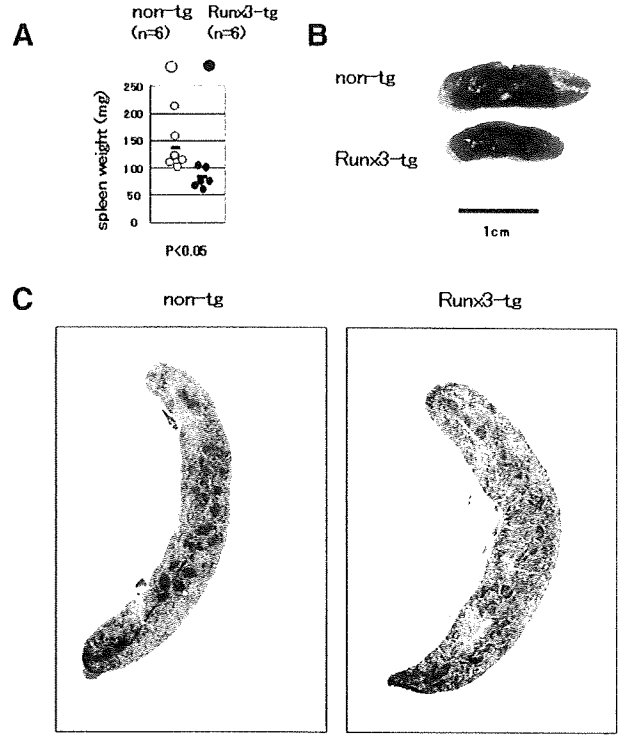

FIGURE 9. Impaired activation of B cells in *Runx3*-transgenic (tg) mice. *A*, Nontransgenic (non-tg) and *Runx3*-transgenic mice were immunized using OVA mixed with aluminum hydroxide, as described for Fig. 8. Animals were sacrificed after the second boosting injection, and the weight of the spleens was measured. Horizontal lines represent the averages of each group. *B*, Representative images of spleens. Bar, 1 cm. *C*, Nontransgenic and *Runx3*-transgenic mice were immunized once with OVA mixed with aluminum hydroxide, and the spleen were removed 1 wk after immunization. Spleen tissue sections were stained using HRP-conjugated peanut agglutinin (brown color).

IgG1 and IgE. However, the production of these two subclasses was poor in *Runx3*-transgenic mice as compared with nontransgenic mice. These results demonstrated that *Runx3*-transgenic mice respond efficiently in a Th1-dependent manner, but that their Th2-mediated response is poor.

B cell activation is impaired in Runx3-transgenic mice

During immunization, we noticed a striking feature of *Runx3*-transgenic mice. When spleens were isolated after a primary challenge of OVA-aluminum, the weight of the tissue was on average 135 mg in nontransgenic mice (Fig. 9, *A* and *B*), whereas the spleen weight in *Runx3*-transgenic mice was 80 mg. This corresponded to ~60% of weight of the nontransgenic spleens. We prepared histological sections of spleens from transgenic and nontransgenic mice, and stained them using peanut agglutinin (Fig. 9*C*). In nontransgenic spleens, a number of lectin-stained clusters were detected, but these clusters were scarcely detectable in *Runx3*-transgenic spleens. Because peanut agglutinin stains B cells in activated germinal centers, these results suggested that B cells were not sufficiently activated in *Runx3*-transgenic spleens following immunization.

Discussion

Runx3 was originally identified as a critical transcription factor in CD8 single-positive thymocyte differentiation that induced *CD8* and repressed *CD4* gene expression (14–16, 25). Recently, a novel function of Runx3 as a feed-forward regulator of T-bet during Th1 cell differentiation of peripheral $CD4^+$ Th cells was described (18). Runx3 is barely detectable in naive $CD4^+$ T cells, but its expression is markedly up-regulated under Th1-skewing conditions. Runx3 induction is dependent on T-bet, and T-bet and Runx3 form a regulatory complex that activates the *IFN-γ* promoter and suppresses *IL-4* expression, at least in part, by binding to an *IL-4* silencer. In agreement with this novel function of Runx3, the derepression of *IL-4* expression is observed in Th1 cells that are deficient in *CBFβ* (26), which has been shown to be necessary for Runx function (27).

Under nonskewed culture conditions, TCR-stimulated $CD4^+$ cells express both T-bet and GATA3. The cells are more or less differentiated along a Th1- or Th2-specific lineage, and the two subpopulations are maintained in a kind of equilibrium. As for GATA3, it is detected even under Th1 conditions, although to a substantially lower extent than Th2. Here, we demonstrated that Runx3 physically interacts with GATA3, and suppresses the transcriptional activity of GATA3. Thus, under nonskewed as well as Th1 conditions, Runx3 appears to negatively regulate Th2 cytokine expression by antagonizing GATA3 activity, contributing to the augmentation or stabilization of Th1 responses. In agreement with this hypothesis, double infection of nonskewed $CD4^+$ cells with retroviruses that expressed Runx3 and GATA3 polarized the cells toward IFN-γ-only or IL-4-only expression, depending on the balance of the two factors. We also demonstrated that *Runx3*-transgenic $CD4^+$ cells were prone to the Th1 phenotype, even in the absence of TCR stimulation. However, *Runx3*-transgenic cells were still able to differentiate along either lineage, given that the introduction of GATA3 or culturing of cells under Th2 conditions could redirect the cells to be IL-4 producers. In *Runx3*-transgenic cells, the protein levels of Runx3 and GATA3 were 1.5-fold higher and 0.7-fold lower, respectively, than in nontransgenic cells. In contrast, in cells in which Runx3 was ectopically overexpressed up to 3.5-fold over wild-type cells, culturing under Th2 conditions failed to restore IL-4 production, which suggests that this level of Runx3 might be above a certain threshold level that can be neutralized by IL-4-induced GATA3. We propose that one mechanism

Downloaded from www.jimmunol.org on February 23, 2010

of regulating the Th1/Th2 preference of TCR-stimulated cells involves the balance of Runx3 and GATA3.

In one sense, the role of Runx3 resembles that of T-bet, which represses *IL-4* expression through a direct association with GATA3 and inhibition of the DNA binding property of GATA3 (9). We demonstrated that *Runx3/I–404*, a Runx3 mutant that is devoid of the Groucho-binding domain, failed to repress *IL-4* expression. Groucho/TLE is an evolutionarily conserved corepressor of Runx family proteins, and functions by recruiting histone deacetylases (28–30). Our results suggest that the repression of *IL-4* expression by the GATA3/Runx3 complex may be mediated through the recruitment of histone deacetylase activity by Groucho.

In nontransgenic Th1 cells, Runx3 was the principal Runx component, and Runx1 was barely detectable. Similarly, naive $CD4^+$ cells isolated from *Runx3*-transgenic mice contained only a trace amount of Runx1. The low level of Runx1 seen in these cells probably reflects the transcriptional repression of the *Runx1* promoter by an excess of the Runx3 transcription factor (31). In contrast, in nontransgenic Th2 cells, equivalent amounts of Runx3 and Runx1 were present. Runx3 in this cell population might prevent the exacerbation of the Th2 response, as was previously suggested for Runx1. We actually obtained results that are in agreement with this notion. When endogenous Runx activity was reduced by introducing dominant negative forms of Runx3, relative expression ratios of IL-4 to IFN-γ under Th2 conditions were substantially enhanced. Runx1 also interacted with GATA3, similar to Runx3 (data not shown), which suggests that the Runx1-GATA3 complex likely exerts a similar biological effect as the Runx3-GATA3 complex.

T cell-specific *Runx3*-deficient mice spontaneously develop asthma-related symptoms, including elevated serum IgE, which is a hallmark of a Th2 bias (26, 32). We showed that *Runx3*-transgenic mice exhibit a Th1-biased phenotype, including elevated titers of serum IgG2a and IgG2b following immunization. These results support the hypothesis that Runx3 is a critical regulator of Th1 and Th2 responses in vivo. A rather unexpected observation in the present study was that B cells failed to respond quickly to immunization in *Runx3*-transgenic mice, as revealed by the poor staining of B cells by peanut agglutinin in *Runx3*-transgenic spleens. Impairment of B cell activation may be due either to the reduction of IL-4 production or an insufficiency of follicular T cells, both of which are crucial factors for B cell activation (33).

Acknowledgments

We thank Dr. S. Akira for *Stat6*-targeted mice, Drs. K. Ito and Y. Ito for Runx3/R178Q plasmid, and M. Kuji for secretarial assistance.

Disclosures

The authors have no financial conflict of interest.

References

1. Mosmann, T. R., H. Cherwinski, M. W. Bond, M. A. Giedlin, and R. L. Coffman. 1986. Two types of murine helper T cell clone. I. Definition according to profiles of lymphokine activities and secreted proteins. *J. Immunol.* 136: 2348–2357.
2. Szabo, S. J., B. M. Sullivan, S. L. Peng, and L. H. Glimcher. 2003. Molecular mechanisms regulating Th1 immune responses. *Annu. Rev. Immunol.* 21: 713–758.
3. Mowen, K. A., and L. H. Glimcher. 2004. Signaling pathways in Th2 development. *Immunol. Rev.* 202: 203–222.
4. Zheng, W., and R. A. Flavell. 1997. The transcription factor GATA-3 is necessary and sufficient for Th2 cytokine gene expression in CD4 T cells. *Cell* 89: 587–596.
5. Ouyang, W., M. Lohning, Z. Gao, M. Assenmacher, S. Ranganath, A. Radbruch, and K. M. Murphy. 2000. Stat6-independent GATA-3 autoactivation directs IL-4-independent Th2 development and commitment. *Immunity* 12: 27–37.
6. Zhu, J., B. Min, J. Hu-Li, C. J. Watson, A. Grinberg, Q. Wang, N. Killeen, J. F. Urban, Jr., L. Guo, and W. E. Paul. 2004. Conditional deletion of Gata3 shows its essential function in T(H)1-T(H)2 responses. *Nat.Immunol.* 5: 1157–1165.
7. Pai, S. Y., M. L. Truitt, and I. C. Ho. 2004. GATA-3 deficiency abrogates the development and maintenance of T helper type 2 cells. *Proc. Natl. Acad. Sci. USA* 101: 1993–1998.
8. Szabo, S. J., S. T. Kim, G. L. Costa, X. Zhang, C. G. Fathman, and L. H. Glimcher. 2000. A novel transcription factor, T-bet, directs Th1 lineage commitment. *Cell* 100: 655–669.
9. Hwang, E. S., S. J. Szabo, P. L. Schwartzberg, and L. H. Glimcher. 2005. T helper cell fate specified by kinase-mediated interaction of T-bet with GATA-3. *Science* 307: 430–433.
10. Kagoshima, H., K. Shigesada, M. Satake, Y. Ito, H. Miyoshi, M. Ohki, M. Pepling, and P. Gergen. 1993. The Runt domain identifies a new family of heteromeric transcriptional regulators. *Trends Genet.* 9: 338–341.
11. Meyers, S., J. R. Downing, and S. W. Hiebert. 1993. Identification of AML-1 and the (8;21) translocation protein (AML-1/ETO) as sequence-specific DNA-binding proteins: the runt homology domain is required for DNA binding and protein-protein interactions. *Mol. Cell. Biol.* 13: 6336–6345.
12. Ito, Y. 2008. RUNX genes in development and cancer: regulation of viral gene expression and the discovery of RUNX family genes. *Adv. Cancer Res.* 99: 33–76.
13. Javed, A., G. L. Barnes, B. O. Jasanya, J. L. Stein, L. Gerstenfeld, J. B. Lian, and G. S. Stein. 2001. runt homology domain transcription factors (Runx, Cbfa, and AML) mediate repression of the bone sialoprotein promoter: evidence for promoter context-dependent activity of Cbfa proteins. *Mol. Cell. Biol.* 21: 2891–2905.
14. Taniuchi, I., M. Osato, T. Egawa, M. J. Sunshine, S. C. Bae, T. Komori, Y. Ito, and D. R. Littman. 2002. Differential requirements for Runx proteins in CD4 repression and epigenetic silencing during T lymphocyte development. *Cell* 111: 621–633.
15. Kohu, K., T. Sato, S. Ohno, K. Hayashi, R. Uchino, N. Abe, M. Nakazato, N. Yoshida, T. Kikuchi, Y. Iwakura, Y. Inoue, et al. 2005. Overexpression of the Runx3 transcription factor increases the proportion of mature thymocytes of the CD8 single-positive lineage. *J. Immunol.* 174: 2627–2636.
16. Sato, T., S. Ohno, T. Hayashi, C. Sato, K. Kohu, M. Satake, and S. Habu. 2005. Dual functions of Runx proteins for reactivating CD8 and silencing CD4 at the commitment process into CD8 thymocytes. *Immunity* 22: 317–328.
17. Komine, O., K. Hayashi, W. Natsume, T. Watanabe, Y. Seki, N. Seki, R. Yagi, W. Sukzuki, H. Tamauchi, K. Hozumi, et al. 2003. The Runx1 transcription factor inhibits the differentiation of naive $CD4^+$ T cells into the Th2 lineage by repressing GATA3 expression. *J. Exp. Med.* 198: 51–61.
18. Djuretic, I. M., D. Levanon, V. Negreanu, Y. Groner, A. Rao, and K. M. Ansel. 2007. Transcription factors T-bet and Runx3 cooperate to activate Ifng and silence Il4 in T helper type 1 cells. *Nat. Immunol.* 8: 145–153.
19. Kanto, S., N. Chiba, Y. Tanaka, S. Fujita, M. Endo, N. Kamada, K. Yoshikawa, A. Fukuzaki, S. Orikasa, T. Watanabe, and M. Satake. 2000. The PEBP2β/CBFβ-SMMHC chimeric protein is localized both in the cell membrane and nuclear subfractions of leukemic cells carrying chromosomal inversion 16. *Leukemia* 14: 1253–1259.
20. Inoue, K., K. Ito, M. Osato, B. Lee, S. C. Bae, and Y. Ito. 2007. The transcription factor Runx3 represses the neurotrophin receptor TrkB during lineage commitment of dorsal root ganglion neurons. *J. Biol. Chem.* 282: 24175–24184.
21. Morita, S., T. Kojima, and T. Kitamura. 2000. Plat-E: an efficient and stable system for transient packaging of retroviruses. *Gene Ther.* 7: 1063–1066.
22. Takeda, K., T. Tanaka, W. Shi, M. Matsumoto, M. Minami, S. Kashiwamura, K. Nakanishi, N. Yoshida, T. Kishimoto, and S. Akira. 1996. Essential role of Stat6 in IL-4 signalling. *Nature* 380: 627–630.
23. Elagib, K. E., F. K. Racke, M. Mogass, R. Khetawat, L. L. Delehanty, and A. N. Goldfarb. 2003. RUNX1 and GATA-1 coexpression and cooperation in megakaryocytic differentiation. *Blood* 101: 4333–4341.
24. Yamashita, M., M. Ukai-Tadenuma, M. Kimura, M. Omori, M. Inami, M. Taniguchi, and T. Nakayama. 2002. Identification of a conserved GATA3 response element upstream proximal from the interleukin-13 gene locus. *J. Biol. Chem.* 277: 42399–42408.
25. Telfer, J. C., E. E. Hedblom, M. K. Anderson, M. N. Laurent, and E. V. Rothenberg. 2004. Localization of the domains in Runx transcription factors required for the repression of CD4 in thymocytes. *J. Immunol.* 172: 4359–4370.
26. Naoe, Y., R. Setoguchi, K. Akiyama, S. Muroi, M. Kuroda, F. Hatam, D. R. Littman, and I. Taniuchi. 2007. Repression of interleukin-4 in T helper type 1 cells by Runx/Cbfβ binding to the Il4 silencer. *J. Exp. Med.* 204: 1749–1755.
27. Wang, Q., T. Stacy, J. D. Miller, A. F. Lewis, T. L. Gu, X. Huang, J. H. Bushweller, J. C. Bories, F. W. Alt, G. Ryan, et al. 1996. The CBFβ subunit is essential for CBFα2 (AML1) function in vivo. *Cell* 87: 697–708.
28. Durst, K. L., and S. W. Hiebert. 2004. Role of RUNX family members in transcriptional repression and gene silencing. *Oncogene* 23: 4220–4224.
29. Wheeler, J. C., C. VanderZwan, X. Xu, D. Swantek, W. D. Tracey, and J. P. Gergen. 2002. Distinct in vivo requirements for establishment versus maintenance of transcriptional repression. *Nat. Genet.* 32: 206–210.
30. Aronson, B. D., A. L. Fisher, K. Blechman, M. Caudy, and J. P. Gergen. 1997. Groucho-dependent and -independent repression activities of Runt domain proteins. *Mol. Cell. Biol.* 17: 5581–5587.
31. Spender, L. C., H. J. Whiteman, C. E. Karstegl, and P. J. Farrell. 2005. Transcriptional cross-regulation of RUNX1 by RUNX3 in human B cells. *Oncogene* 24: 1873–1881.
32. Fainaru, O., E. Woolf, J. Lotem, M. Yarmus, O. Brenner, D. Goldenberg, V. Negreanu, Y. Bernstein, D. Levanon, S. Jung, and Y. Groner. 2004. Runx3 regulates mouse TGF-beta-mediated dendritic cell function and its absence results in airway inflammation. *EMBO J.* 23: 969–979.
33. King, C., S. G. Tangye, and C. R. Mackay. 2008. T follicular helper (TFH) cells in normal and dysregulated immune responses. *Annu. Rev. Immunol.* 26: 741–766.

Downloaded from www.jimmunol.org on February 23, 2010

CD69 Controls the Pathogenesis of Allergic Airway Inflammation[1]

Takako Miki-Hosokawa,[2]*† Akihiro Hasegawa,[2]*† Chiaki Iwamura,[2]* Kenta Shinoda,* Soichi Tofukuji,* Yukiko Watanabe,* Hiroyuki Hosokawa,* Shinichiro Motohashi,* Kahoko Hashimoto,‡ Mutsunori Shirai,† Masakatsu Yamashita,* and Toshinori Nakayama[3]*

Airway inflammation and airway hyperresponsiveness are central issues in the pathogenesis of asthma. CD69 is a membrane molecule transiently expressed on activated lymphocytes, and its selective expression in inflammatory infiltrates suggests that it plays a role in the pathogenesis of inflammatory diseases. In CD69-deficient mice, OVA-induced eosinophilic airway inflammation, mucus hyperproduction, and airway hyperresponsiveness were attenuated. Cell transfer of Ag-primed wild-type but not CD69-deficient CD4 T cells restored the induction of allergic inflammation in CD69-deficient mice, indicating a critical role of CD69 expressed on CD4 T cells. Th2 responses induced by CD69-deficient CD4 T cells in the lung were attenuated, and the migration of CD4 T cells into the asthmatic lung was severely compromised. The expression of VCAM-1 was also substantially altered, suggesting the involvement of VCAM-1 in the CD69-dependent migration of Th2 cells into the asthmatic lung. Interestingly, the administration of anti-CD69 Ab inhibited the induction of the OVA-induced airway inflammation and hyperresponsiveness. This inhibitory effect induced by the CD69 mAb was observed even after the airway challenge with OVA. These results indicate that CD69 plays a crucial role in the pathogenesis of allergen-induced eosinophilic airway inflammation and hyperresponsiveness and that CD69 could be a possible therapeutic target for asthmatic patients. ***The Journal of Immunology,*** **2009, 183: 8203–8215.**

Asthma is a chronic inflammatory disease of the lower airways that causes airway hyperresponsiveness (AHR)[4] to a wide variety of specific and nonspecific stimuli (1, 2). In most cases, the extent of AHR correlates with the level of airway inflammation. Hallmarks of asthma include airway inflammation predominated by eosinophils, mucus hyperproduction, and Th2 cytokines (IL-4, IL-5, and IL-13) (3–7). A suggestion for a Th2 paradigm for allergic diseases, wherein increased activation of Th2 cells that produce Th2 cytokines results in IgE production and the recruitment and activation of eosinophils, comes from observations of animal models previously studied. This notion has been supported by clinical studies in which the release of Th2-like cytokines from the lymphocytes of asthmatic patients was demonstrated (8, 9).

CD69 is a type II membrane protein expressed as a homodimer composed of heavily glycosylated subunits (10). CD69 is known as an early activation marker Ag of lymphocytes (11, 12). Freshly prepared thymocytes undergoing selection events express CD69, and regulatory roles for CD69 expression in T cell development in the thymus have been suggested (13, 14). The regulatory roles of CD69 in a collagen-induced arthritis model (15) and an anti-collagen Ab-induced arthritis model (16) were reported and multiple target processes were suggested; however, the role of CD69 in other inflammatory models, such as in the allergic airway inflammation, has not been clarified. More recently, a new function of CD69 in the lymphocyte trafficking has been proposed (17).

We herein investigated the role of CD69 using a mouse model of allergic asthma and found that CD69 plays a critical role in the induction of both Ag-induced eosinophilic airway inflammation and AHR. Furthermore, administration of anti-CD69 Ab resulted in a dramatic reduction in the extent of airway inflammation and AHR, suggesting that the CD69 mAb could be used for the treatment of asthmatic patients.

Materials and Methods

Mice

CD69-deficient (CD69KO) mice (16) were backcrossed with BALB/c 10 times. BALB/c and C57BL/6 mice were purchased from Charles River Laboratories. GFP-transgenic (Tg) mice with a C57BL/6 background expressed an enhanced GFP in all tissue under the control of the β-actin promoter (18). All mice including OVA-specific αβ-TCR-transgenic (DO11.10 Tg) mice (19) were maintained under specific pathogen-free conditions. All animal care was conducted in accordance with the guidelines of Chiba University.

*Department of Immunology, Graduate School of Medicine, Chiba University, Chiba, Japan; †Department of Microbiology and Immunology, Yamaguchi University School of Medicine, Yamaguchi, Japan; and ‡Department of Life and Environmental Sciences and High Technology Research Center, Chiba Institute of Technology, Chiba Japan

Received for publication February 26, 2009. Accepted for publication October 9, 2009.

The costs of publication of this article were defrayed in part by the payment of page charges. This article must therefore be hereby marked *advertisement* in accordance with 18 U.S.C. Section 1734 solely to indicate this fact.

[1] This work was supported by the Global Center of Excellence Program (Global Center for Education and Research in Immune System Regulation and Treatment), MEXT (Monbukagakusho) (Japan), and by grants from the Ministry of Education, Culture, Sports, Science and Technology (Japan) (Grants-in-Aid for Scientific Research on Priority Areas nos. 17016010 and 20060003, Scientific Research (B) no. 17390139, Scientific Research (C) nos. 18590466, 19590491, 19591609, and 20590485, Exploratory Research no. 19659121, and Young Scientists (B) no. 20790367, (Start-up) 20890038: Special Coordination Funds for Promoting Science and Technology, and Cancer Translational Research Project), the Ministry of Health, Labor and Welfare (Japan), and The Japan Health Science Foundation. This work was also supported by the Naito Foundation.

[2] T.M.-H., A.H., and C.I. contributed equally to this work.

[3] Address correspondence and reprint request to Dr. Toshinori Nakayama, Department of Immunology, Graduate School of Medicine, Chiba University, 1-8-1 Inohana, Chuo-ku, Chiba 260-8670 Japan. E-mail address: tnakayama@faculty.chiba-u.jp

[4] Abbreviations used in this paper: AHR, airway hyperresponsiveness; BAL, bronchioalveolar lavage; Cdyn, dynamic compliance; PAS, periodic acid-Schiff; RL, lung resistance; $S1P_1$, sphingosine 1 phosphate receptor 1; Tg, transgenic; KO, knockout; WT, wild type; HPRT, hypoxanthine phosphoribosyltransferase; Penh, enhanced pause.

Copyright © 2009 by The American Association of Immunologists, Inc. 0022-1767/09/$2.00

www.jimmunol.org/cgi/doi/10.4049/jimmunol.0900646

Downloaded from www.jimmunol.org on February 23, 2010

Immunofluorescent staining and flow cytometric analysis

In general, one million cells were incubated on ice for 30 min with the appropriate staining reagents according to a standard method (20). Intracellular staining of IL-4 and IFN-γ was performed as described previously (21). FITC-conjugated anti-IFN-γ Ab (XMG1.2), PE-conjugated anti-IL-4 Ab (11B11), PE-conjugated anti-KJ1-26 Ab, and allophycocyanin-conjugated anti-CD4 Ab (RM4-5; all from BD Biosciences) were used for detection.

OVA sensitization and OVA inhalation

CD69-deficient and wild-type (WT) BALB/c or C57BL/6 mice were immunized i.p. with 250 μg of OVA (chicken egg albumin from Sigma-Aldrich) in 4 mg of aluminum hydroxide gel (alum) on days 0 and 7. Where indicated, we used 50 μg of OVA in 2 mg of alum. Mice inhaled aerosolized 1% OVA in saline for 30 min using a supersonic nebulizer (model NE-U07; Omron) on days 14 and 16 to assess the degree of eosinophilic inflammation and AHR. In some experiments, mice were immunized on days 0 and 7 and received intranasal OVA (100 μg) challenges on days 14 and 16.

Collection and analysis of bronchioalveolar lavage (BAL) fluid

One day after the last OVA inhalation (on day 17), BAL was performed as previously described (22). All of the BAL fluid was collected and cells in 150-μl aliquots were counted. One hundred thousand viable BAL cells were cytocentrifuged onto slides by a Cytospin4 (Shandon) and stained with May-Grünwald Giemsa solution (Merck). Five hundred leukocytes were counted on each slide. Cell types were identified using morphological criteria. The percentages of each cell type were calculated.

Lung histology and immunohistochemistry

Mice were sacrificed by CO_2 asphyxiation 24 h after the last OVA inhalation on day 17 and the lungs were infused with 10% (v/v) formalin in PBS for fixation. The samples were sectioned and stained with Luna and periodic acid-Schiff (PAS) stain for the examination of pathological changes under a light microscope at ×100 or ×200 as described previously (22). The number of infiltrated mononuclear cells in the perivascular and peribronchiolar regions was determined by direct counting of three different fields per slide. The numerical scores for the abundance of PAS-positive mucus-containing cells in each airway were determined as follows: 0, <0.5% PAS-positive cells; 1, 5–25%; 2, 25–50%; 3, 50–75%; and 4, >75% as described elsewhere (23).

Cytokine and chemokine expression in asthmatic lung tissue, BAL fluid, and lung CD4 T cells assessed by quantitative RT-PCR

Total RNA was isolated from the lung (three mice in each group) using the TRIzol reagent (Sigma-Aldrich). Reverse transcription was conducted with Superscript II RT (Invitrogen). The total BAL fluid was collected 1 day after the last OVA inhalation. CD4 T cells were purified by cell sorting, and the levels of expression of cytokines and chemokines were analyzed. Whole lung mononuclear cells were stimulated with OVA for 24 h, and CD4 T cells were subsequently collected by cell sorting. Quantitative RT-PCR was performed as described previously (24, 25). The primers for TaqMan probes for the detection of IL-4, IL-5, IL-13, IFN-γ, eotaxin 2, Gob-5 and Muc-5ac, and hypoxanthine phosphoribosyltransferase (HPRT) were purchased from Applied Biosystems. The expression was normalized by the HPRT signal.

Measurement of AHR

AHR was assessed 1 day after the last OVA inhalation by methacholine-induced airflow obstruction of conscious mice placed in a whole-body plethysmograph (model PLY3211; Buxco Electronics) as previously described (22). The respiratory parameters were obtained by exposing mice to 0.9% saline mist, followed by incremental doses of aerosolized methacholine. Airflow obstruction was monitored and analyzed by system XA software (model SFT3410; Buxco Electronics). The results are expressed as the average percentage of baseline enhanced pause (Penh) values after 0.9% saline exposure. Airway function was further assessed by measuring the changes in lung resistance (RL) and dynamic compliance (Cdyn) in response to increasing doses of inhaled methacholine (26–28). The maximum values of RL and Cdyn were taken and expressed as the percentage change from baseline after saline aerosol exposure.

Adoptive transfer of CD4 T cells

Splenic CD4 T cells of OVA-sensitized WT or CD69-deficient mice were purified using a $CD4^+$ T cell isolation kit (Miltenyi Biotec) and AutoMACS sorter (Miltenyi Biotec), yielding a purity of >98%. These cells were administered i.v. through the tail vein to OVA-sensitized CD69-deficient mice (1×10^7 cells/mouse) 1 day before the first airway challenge with aerosolized OVA (day 13). After cell transfer, the mice were exposed to allergen challenges via the airway on days 14 and 16 and assays were conducted on day 17.

Adoptive transfer of CD69-overexpressed Th2 cells

Naive CD4 T cells from DO11.10 Tg WT or CD69-deficient mice were stimulated with immobilized anti-TCR plus anti-CD28 mAb under Th2 conditions. On day 2, the mouse *CD69* (m*CD69*) gene was introduced by a retrovirus vector containing the m*CD69* gene (29). On day 5, the cultured cells were harvested and one or three million cells ($KJ1^+$ Th2 cells) were injected i.v. into normal BALB/c mice.

In vitro Th2 cell differentiation cultures

DO11.10 Tg $CD44^{low}CD4^+$ T cells (1.5×10^4) purified by cell sorting were stimulated with antigenic OVA peptide (Loh 15) and irradiated (3500 rad) T cell-depleted BALB/c APCs. The cultured cells were restimulated with immobilized anti-TCR-β mAb for 48 h, and the concentrations of cytokines in the supernatant were assessed by ELISA (21).

Visualization of OVA-primed CD4 T cells infiltrated into the lung after OVA inhalation

WT and CD69-deficient mice were immunized i.p. with 250 μg of OVA-alum on days 0 and 7. Splenic CD4 T cells were purified using a CD4 T cell isolation kit and a MACS sorter. The CD4 T cells were stained with either CFDA-SE (4 μM) or SNARF-1 (5 μM; Invitrogen) at 37°C for 15 min. Where indicated, GFP Tg mice (C57BL/6 background) were immunized with OVA and splenic CD4 T cells were purified using a CD4 T cell isolation kit and a MACS sorter. These CD4 T cells were administrated i.v. through the tail vain to normal C57BL/6 mice 24 h before OVA inhalation. One or 2 days after the last OVA inhalation, transferred T cells were monitored using a Leica M205FA fluorescence microscope equipped with a Keyence VB-7010 charge-coupled device (CCD) color camera system (30).

Assessment of the expression of VCAM-1 in the asthmatic lung

The lungs were fixed with in 4% paraformaldehyde (WAKO) after extensive washing. The tissues were embedded in Tissue-Tek OCT compound (Sakura Fine Technical). For microscopic analysis, an Alexa Fluor SFX kit (Invitrogen) was used according to the manufacturer's instructions. In brief, 10-μm cryostat sections were washed with PBS. Sections were blocked with Image-iT Fx Signal Enhancer for 30 min at room temperature and stained with rabbit anti-VCAM-1 Ab (H-276; Santa Cruz Biotechnology) in PBS containing 2% FCS for 15 h at 4°C. After washing with PBS, sections were treated with Alexa Fluor 555 goat anti-rabbit Ab for 3 h at room temperature. The specimen was analyzed using fluorescence microscopy (BZ-9000; Keyence) (31).

Anti-CD69 Ab treatment

BALB/c mice were immunized i.p. with 250 μg of OVA-alum on days 0 and 7. Twenty-four hours before the first airway challenge by OVA inhalation (on day 13), mice were injected i.p. with anti-CD69 mAb (H1.2F3, 250 or 500 μg/mouse). The mice were exposed to allergen challenges on days 14 and 16 and assays were conducted on day 17. Where indicated, anti-CD69 mAb was injected just after the second OVA challenge and BAL fluid was examined on days 17, 19, and 21. In one experiment (shown in Fig. 7), recipient mice transferred with GFP Tg CD4 T cells were challenged by OVA inhalation on day 15 and anti-CD69 mAb were injected 1 h before inhalation or 1day after inhalation, and the assay was conducted on day 17.

Statistical analysis

The Student *t* test was used.

Results

Attenuated OVA-induced eosinophilic inflammation and AHR in CD69-deficient mice

The aim of this study was to evaluate the role of CD69 in the development of allergic airway inflammation and AHR. WT and

Downloaded from www.jimmunol.org on February 23, 2010

CD69-deficient mice were sensitized with OVA-alum on days 0 and 7 and subsequently received an OVA inhalation on days 14 and 16 (Fig. 1*A*). The expression of CD69 was induced in infiltrating leukocytes in WT animals after the OVA sensitization and challenge (data not shown). One day after the last inhalation, the BAL fluid was harvested and examined for infiltrating leukocytes. A summary of the infiltrated cell types is shown in Fig. 1*B*. The frequencies of eosinophils in the BAL fluid samples were lower in CD69-deficient mice in comparison to WT mice. The lung sections were subjected to Luna staining and the perivascular and peribronchiolar regions were assessed for eosinophilic infiltration (Fig. 1*C*). The number of infiltrated eosinophils was significantly reduced in the CD69-deficient mice in comparison to the WT after receiving the OVA airway challenge. Next, the levels of mRNA expression of Gob-5 and Muc-5ac, molecular makers for goblet cell hyperplasia and mucus production, were assessed in the lungs of CD69-deficient mice (Fig. 1, *D* and *E*). As expected, Gob-5 and Muc-5ac expression levels were reduced in the CD69-deficient mice in comparison to the WT. The AHR as measured by methacholine-induced airflow obstruction with a whole-body plethysmograph was not obviously observed in the OVA-sensitized and OVA-challenged CD69-deficient mice (CD69KO/OVA) in comparison to the WT mice (WT/OVA) (Fig. 1*F*).

To further examine the role of CD69 in the pathogenesis of allergic asthma, we used a different experimental asthma model wherein WT and CD69-deficient mice were immunized i.p. and challenged intranasally with OVA (24). The numbers of total infiltrated leukocytes and eosinophils in the BAL fluid were all significantly decreased (Fig. 1*G*), and the level of AHR was dramatically reduced (Fig. 1*H*) in the CD-69-deficient mice compared with WT. Similar results were obtained by the experiments using low-dose OVA-sensitization and OVA challenge (Fig. 1*I*). Our results indicate that the OVA-induced airway inflammation and AHR are therefore attenuated in CD69-deficient mice.

Attenuated Th2 responses induced by CD69-deficient CD4 T cells in the lung

We next examined the mRNA expression levels of IL-4, IL-5, IL-13, IFN-γ, eotaxin 2, IL-2, and TNF-α in CD4 T cells in the BAL fluid of OVA-sensitized and OVA-challenged CD69-deficient mice shown in Fig. 1. CD4 T cells in the BAL fluid were purified by cell sorting and RNA was subsequently prepared. Although the mRNA levels of IL-4, IFN-γ, IL-2, and TNF-α were not significantly changed, there was a substantial decrease in the expression of IL-5, IL-13, and eotaxin 2 in the CD69-deficient mice (Fig. 2*A*). Lung mononuclear cells from OVA-sensitized and OVA-challenged CD69-deficient mice were stimulated in vitro with OVA for 24 h, and the CD4 T cells were subsequently purified by cell sorting. A dramatic decrease in the mRNA expression of IL-4, IL-5, and IL-13 and a moderate decrease in eotaxin 2 were observed in the lung CD4 T cells from CD69-deficient mice after Ag stimulation in vitro (Fig. 2*B*). Spleen cells and BAL fluid mononuclear cells from OVA-sensitized and OVA-challenged CD69-deficient mice were stimulated in vitro with PMA and ionomycin for 4 h, and intracellular IFN-γ/IL-4 profiles of CD4 T cells were assessed. Although the number of IL-4-producing Th2 cells recovered from the spleen was not significantly changed, a substantial decrease in the number of Th2 cells in the BAL fluid was seen in the CD69-deficient mice (Fig. 2*C*). These results suggest that functional Th2 cell numbers in the lung were reduced in the inflamed lung of CD69-deficient mice.

We then examined the efficiency of Th2 cell differentiation using OVA-specific DO11.10 TCR Tg CD69-deficient CD4 T cells in vitro (Fig. 2*D*). Intracellular IFN-γ/IL-4 profiles revealed that the number of IL-4-producing Th2 cells was lower in the CD69-deficient groups at all Ag doses. The production of IL-4, IL-5, IL-13, and IFN-γ in the culture supernatant of the in vitro differentiated Th2 cells was also measured and moderate reduction of the production of Th2 cytokines was seen in the CD69-deficient DO11.10 Tg Th2 cells (Fig. 2*E*). Th2 cell survival in the in vitro culture was not significantly altered in the absence of CD69 expression (data not shown). Thus, the attenuated OVA-induced airway inflammation and AHR observed in CD69-deficient mice could be in part due to the weaker Th2 responses induced by CD69-deficient Th2 cells in the lung.

Requirement of CD69 on Ag-primed CD4 T cells in the induction of eosinophilic airway inflammation and AHR

To investigate the cellular basis underlying the requirement of CD69 in the pathogenesis of allergic asthma, we performed cell transfer experiments in which splenic CD4 T cells from OVA-primed WT and CD69-deficient mice were adoptively transferred into OVA-sensitized CD69-deficient mice (Fig. 3*A*). As shown in Fig. 3*B*, eosinophilic infiltration was restored by the transfer of OVA-primed WT CD4 T cells into the CD69-deficient mice. Luna staining revealed that the transfer of OVA-primed WT CD4 T cells (Fig. 3*C*) resulted in substantial restoration of the infiltration of eosinophils in the perivascular and peribronchiolar regions, whereas transfer of unprimed WT CD4 T cells or primed CD69-deficient CD4 T cells failed to restore the eosinophilic infiltration. Similarly, the development of AHR was observed upon transfer of OVA-primed WT CD4 T cells into CD69-deficient mice (Fig. 3*D*). The restoration of the AHR was confirmed by a direct measurement of RL and Cdyn in anesthetized, tracheostomized, intubated, and mechanically ventilated CD69-deficient mice (Fig. 3, *E* and *F*). Furthermore, CD69-deficient mice responded with mucus hyperproduction when they received OVA-primed WT $CD4^+$ T cells (Fig. 3, *G* and *H*). Allergic inflammation and AHR were induced, although to a relatively milder extent, when OVA-primed WT CD4 T cells were transferred into nonsensitized CD69-deficient mice, and the extent of disease was reduced in the CD69-deficient CD4 T cell groups (data not shown). These results indicate that CD69 molecules on Ag-primed CD4 T cells play an important role in the induction of eosinophilic airway inflammation and AHR.

CD69-overexpressed Th2 cells restored the defect in the induction of eosinophilic inflammation of CD69-deficient Th2 cells

To further investigate whether the eosinophilic airway inflammation is dependent on the expression of CD69 on Th2 cells, OVA-specific TCR$\alpha\beta$ Tg (DO11.10 Tg) CD69-deficient CD4 T cells were cultured under Th2 conditions for 2 days and the developing Th2 cells were infected with a retrovirus vector containing the mouse *CD69* gene (Fig. 4*A*). The overexpression of CD69 was confirmed (Fig. 4*B*). The CD69-overexpressed Th2 cells (3×10^6) were transferred to normal BALB/c recipient mice and after 1 and 3 days, the recipient mice were challenged by OVA inhalation, and the BAL fluid was collected on day 10. As shown in Fig. 4*C*, eosinophilic infiltration was lower in mice receiving CD69-deficient DO11.10 Tg Th2 cells (CD69 KO mock infected) compared with those receiving WT Th2 cells (WT mock infected). Eosinophilic infiltration was restored in the mice that received CD69-overexpressed Th2 cells (CD69 mCD69 infected). These results indicate that overexpression of CD69 overcame the defect in the induction of allergic eosinophilic inflammation of CD69-deficient Th2 cells.

Downloaded from www.jimmunol.org on February 23, 2010

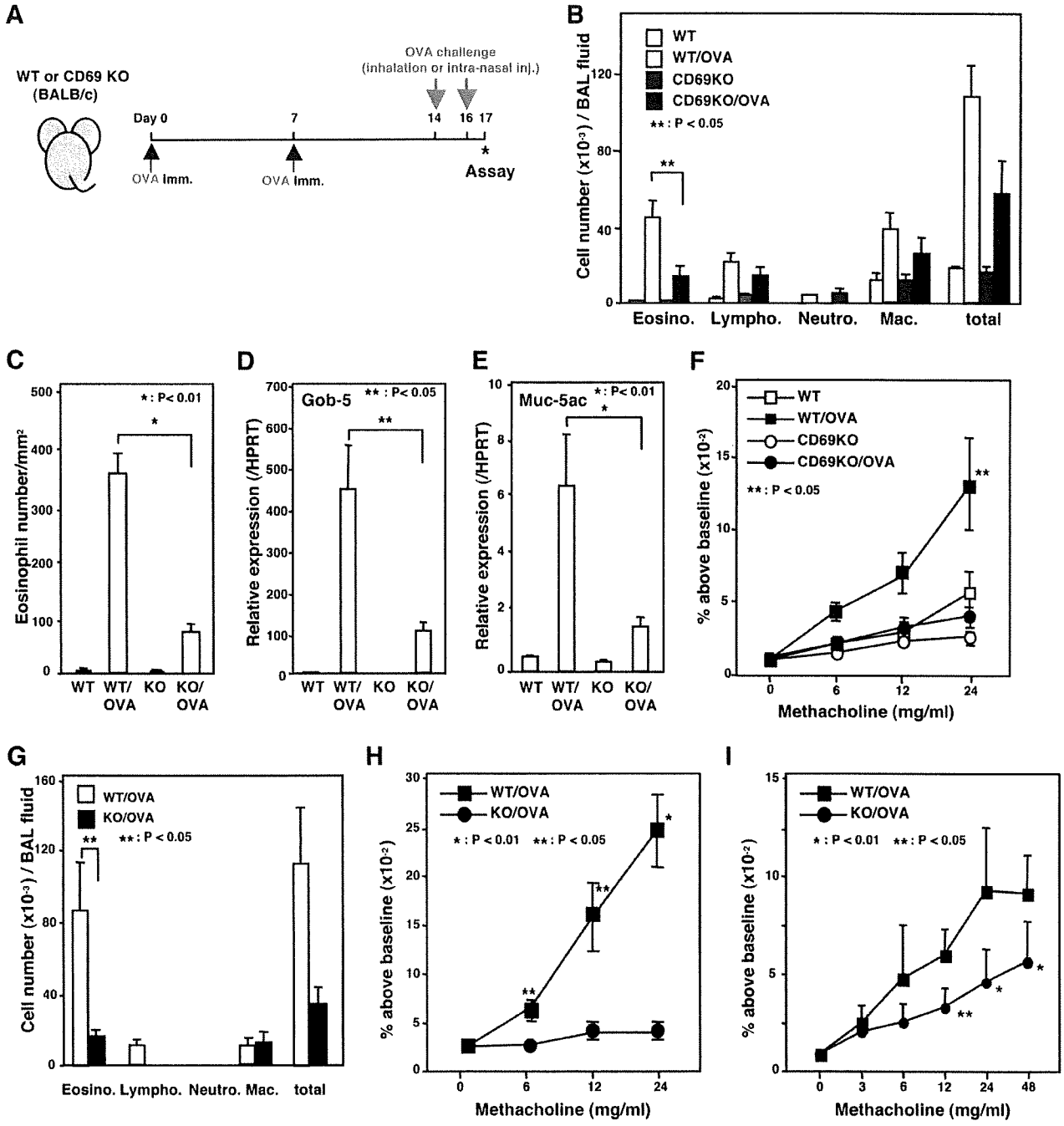

FIGURE 1. Inhibition of OVA-induced eosinophilic inflammation and AHR in CD69-deficient mice. *A*, Six-week-old WT or CD69-deficient (CD69 KO) mice were sensitized with OVA-alum and were subsequently challenged with or without OVA on days 14 and 16. One day after the last challenge, assays were performed. *B*, OVA-induced eosinophilic infiltration in the BAL fluid. Six- week-old WT and CD69-deficient mice were sensitized with OVA-alum and were subsequently challenged with (WT/OVA or CD69KO/OVA) or without (WT or CD69KO) OVA on days 14 and 16. One day after the last challenge, the mice were sacrificed and the BAL fluid was collected. The absolute cell numbers of eosinophils (Eosino.), lymphocytes (Lympho.), neutrophils (Neutro.), and macrophages (Mac.) are shown with the SEM. Four mice from each group were used in this experiment. **, $p < 0.05$. *C*, The lung tissue specimens were fixed and stained with Luna. The number of peribronchiolar eosinophilic infiltrates is shown with the SEM. *, $p < 0.01$. *D* and *E*, mRNA expression of Gob-5 (*D*) and Muc-5ac (*E*) in the lung tissue was determined by quantitative RT-PCR. The relative intensity (/HPRT signal, mean of three samples) is shown with SDs. *F*, One day after the last OVA challenge, AHR in response to increasing doses of methacholine was measured in a whole-body plethysmograph. The mean values of the percent above baseline are shown with the SEM for four mice. A total of five independent experiments was performed with similar results. **, $p < 0.05$ (between WT/OVA and CD69KO/OVA groups). *G*, OVA-sensitized CD69-deficient mice were challenged intranasally with 100 μg of OVA twice while under anesthesia on days 14 and 16. One day after the last challenge, the mice were sacrificed and the BAL fluid was collected. The absolute cell number of eosinophils (Eosino.), lymphocytes (Lympho.), neutrophils (Neutro.), and macrophages (Mac.) are shown with the SEM. Four mice from each group were used in this experiment. **, $p < 0.05$. *H*, AHR was monitored by measuring Penh. Mean values of the percent above baseline are shown with SDs of four mice. *, $p < 0.01$ and **, $p < 0.05$. *I*, CD69-deficient mice were immunized i.p. with 50 μg in 2 mg of alum on day 0 and were subsequently challenged intranasally with 30 μg of OVA on days 7, 8, and 9. One day after the last challenge, AHR was monitored by measuring RL. Mean values of the percent above baseline are shown with SDs of four mice. *, $p < 0.01$ and **, $p < 0.05$.

Downloaded from www.jimmunol.org on February 23, 2010

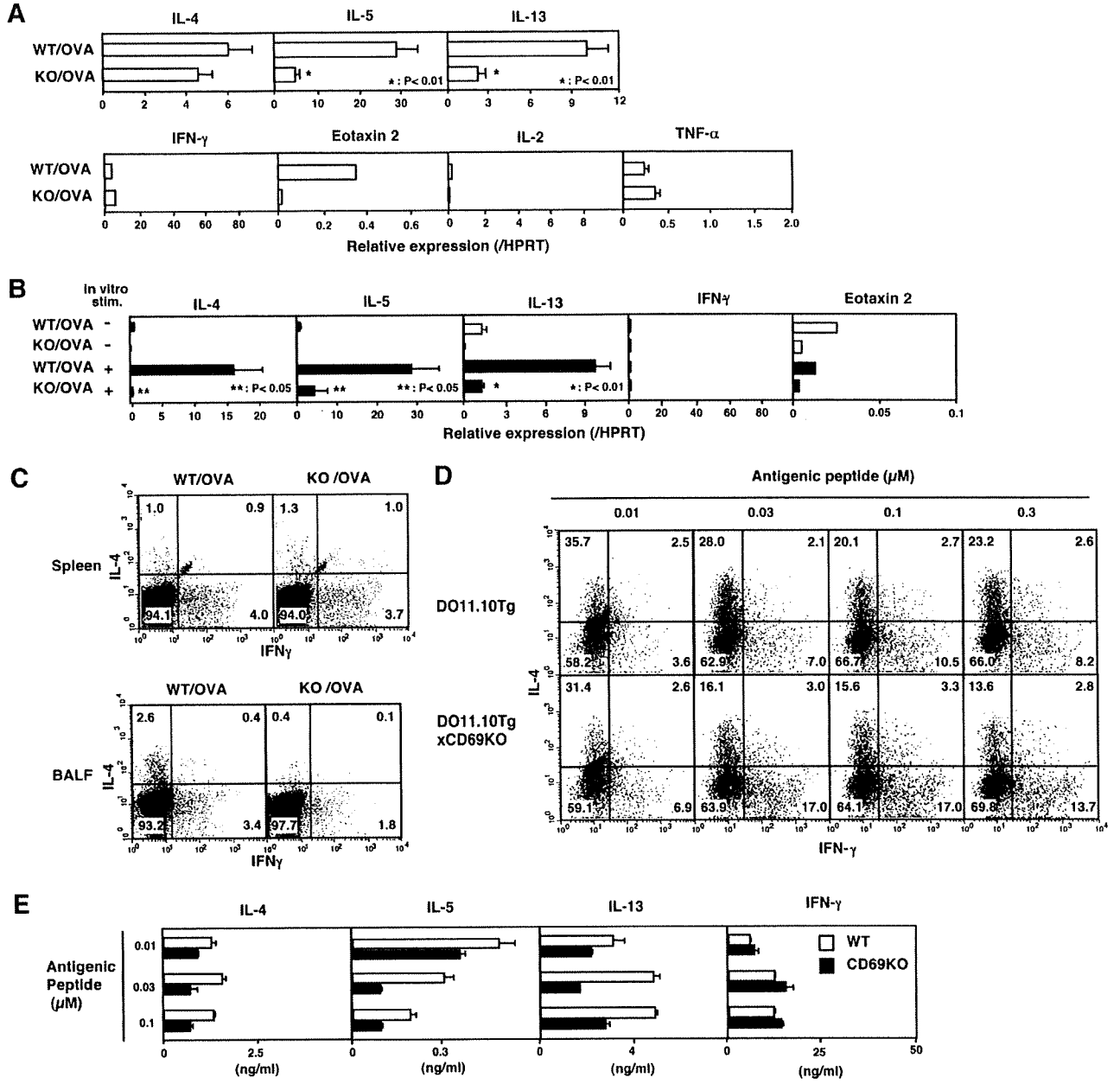

FIGURE 2. Decreased Th2 responses induced by CD69-deficient CD4 T cells. *A*, mRNA expression of IL-4, IL-5, IL-13, IFN-γ, eotaxin2, IL-2, and TNF-α in CD4 T cells in the BAL fluid. CD4 T cells in the BAL fluid were obtained from OVA-sensitized and OVA-challenged CD69-deficient mice 1 day after the last OVA inhalation, and the levels of mRNA expression of the indicated cytokines and a chemokine were determined by quantitative RT-PCR. The mean values of four samples are shown with SDs. *B*, mRNA expression of IL-4, IL-5, IL-13, IFN-γ, and eotaxin 2 expression in lung CD4 T cells. Whole lung mononuclear cells obtained from OVA-sensitized and OVA-challenged CD69-deficient mice were stimulated in vitro with antigenic OVA for 24 h. The $CD4^+$ T cells were collected by cell sorting, and the levels of mRNA expression of the indicated cytokines and a chemokine were determined by quantitative RT-PCR. The mean values of four samples are shown with SDs. *C*, Intracellular IFN-γ/IL-4 profiles of CD4 T cells from the spleen and BAL fluid mononuclear cells. Spleen cells and BAL fluid mononuclear cells obtained from OVA-sensitized and OVA-challenged CD69-deficient mice were stimulated in vitro with PMA and ionomycin for 4 h, and intracellular IFN-γ/IL-4 profiles of CD4 T cells were examined. The percentages from each quadrant are also shown. *D*, OVA-specific TCR Tg (DO11.10 TCR Tg) naive CD4 T cells were stimulated with increasing doses of antigenic peptides (0.01–0.3 μM) and irradiated APCs. Five days later, the cells were restimulated with immobilized anti-TCR mAb for 6 h, and intracellular IFN-γ/IL-4 profiles were examined. The percentages from each quadrant are also shown. Three independent experiments were performed with similar results. *E*, Cytokine production was assessed using in vitro-differentiated Th2 cells as in *C*. Mean values are shown with SDs ($n = 5$).

Impaired migration of CD69-deficient T cells into the asthmatic lung

To evaluate the ability of CD69-deficient CD4 T cells to migrate into the inflamed lung tissue, we used color-coded lymphocytes and an imaging model to visualize the migration of OVA-specific Th2 cells into the lung after allergen inhalation. WT and CD69-deficient mice were immunized with OVA on days 0 and 7, and the spleen CD4 T cells were stained with either CFDA-SE or SNARF-1. CFDA-SE-labeled WT CD4 T cells (2×10^7) and SNARF-1-labeled CD69KO T cells (2×10^7)

Downloaded from www.jimmunol.org on February 23, 2010

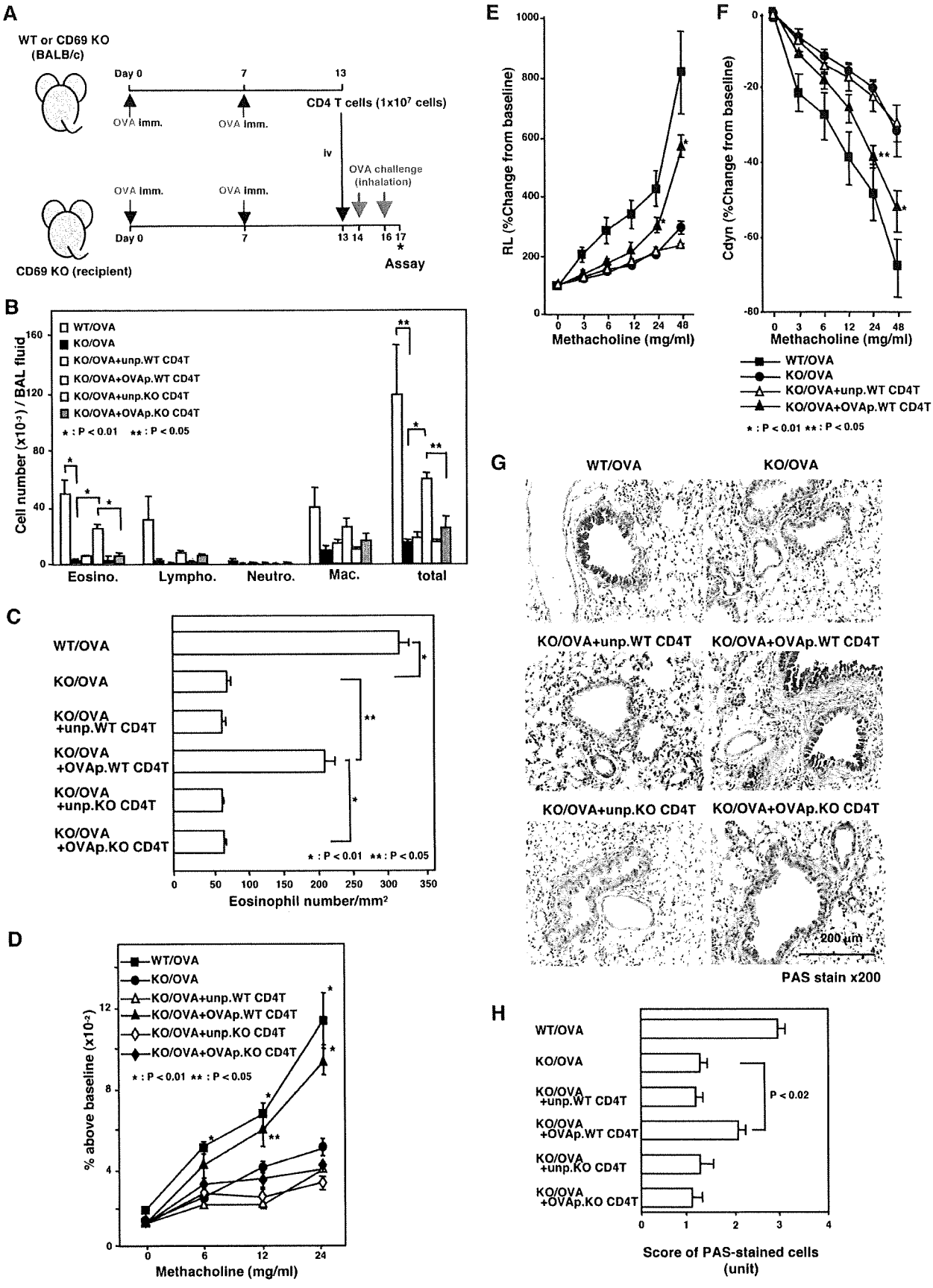

Downloaded from www.jimmunol.org on February 23, 2010

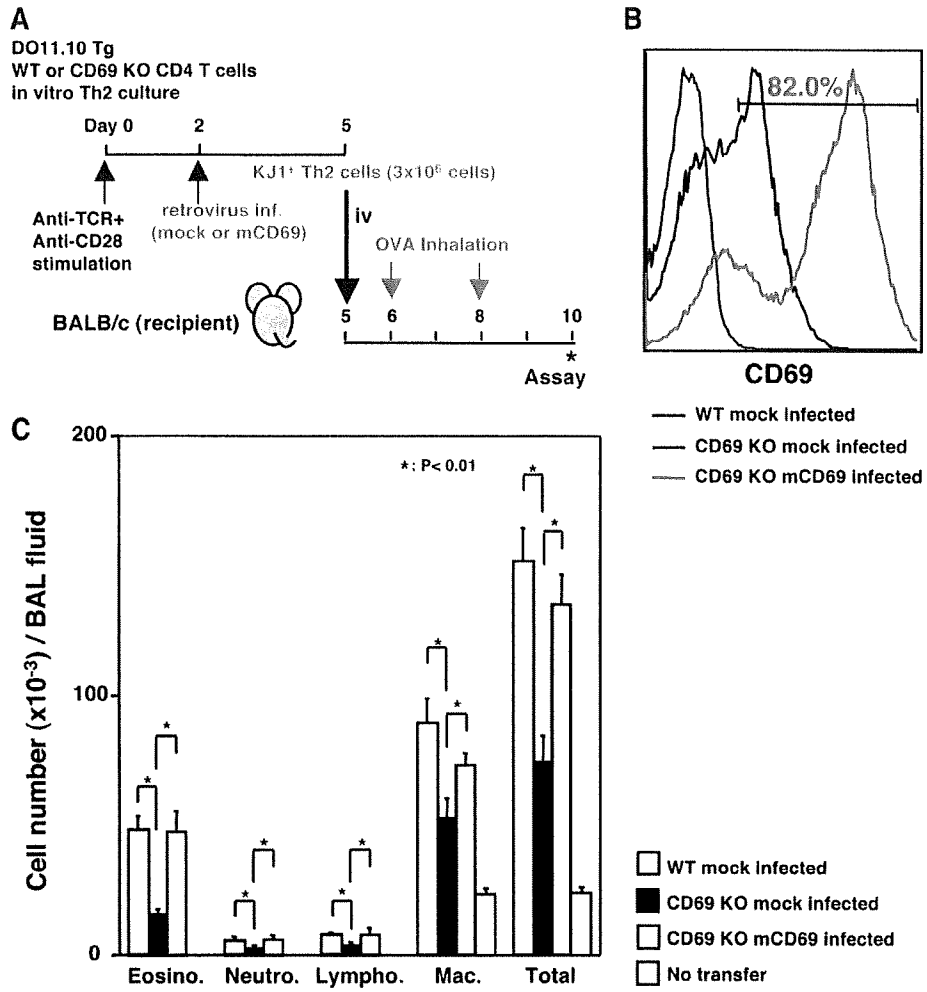

FIGURE 4. Induction of airway inflammation in CD69-deficient mice following adoptive transfer of CD69-overexpressing T cells. *A*, A schematic overview of the study protocol for the induction of asthma. Naive CD4 T cells from DO11.10 Tg WT or CD69-deficient (CD69KO) mice were stimulated with immobilized anti-TCR plus anti-CD28 mAb under Th2 conditions. On day 2, the mouse CD69 (mCD69) gene was introduced by a retrovirus vector containing the mCD69 gene. On day 5, the cultured cells were harvested and one or three million cells ($KJ1^+$ Th2 cells) were injected i.v. into normal BALB/c mice. The recipient mice were exposed to airway challenge with aerosolized OVA on days 6 and 8. BAL fluid was collected on day 10. *B*, A representative CD69 expression profile of the transferred $CD4^+$ Th2 cells (WT mock infected, CD69 KO mock infected, and CD69 KO mCD69 infected). The proportion of CD69-overexpressing cells in the CD69 KO mCD69-infected CD4 T cells was also indicated. *C*, Two days after the last OVA inhalation, the mice were sacrificed and the BAL fluid was collected. Cells in the BAL fluid were analyzed as in Fig. 1*A*. The absolute cell numbers of eosinophils (Eosino.), lymphocytes (Lympho.), neutrophils (Neutro.), and macrophages (Mac.) are shown with the SEM. Five mice from each group were used in this experiment. *, $p < 0.01$. Three independent experiments with titration of transferred cells were performed and similar results were obtained.

were mixed and i.v. transferred into normal syngeneic C57BL/6 mice. One day later, the recipient mice were challenged by OVA inhalation (Fig. 5*A*). The mice were sacrificed and the excised lungs were examined using a Leica M205FA fluorescence microscope equipped with a Keyence VB-7010 CCD color camera system as described in *Materials and Methods*. This system allows us

FIGURE 3. OVA-induced eosinophilic inflammation and AHR were restored by adoptive transfer of OVA-primed WT but not CD69-deficient CD4 T cells. *A*, Splenic CD4 T cells from OVA-sensitized WT or CD69-deficient mice were administered i.v. into OVA-sensitized CD69-deficient mice (1×10^7 cells/mouse) 1 day before the first airway OVA challenge (day 13). The recipient mice were exposed to OVA challenges by inhalation on days 14 and 16. All assays were performed on day 17. *B*, We analyzed the cells in the BAL fluid from WT (WT/OVA), CD69-deficient (KO/OVA) mice without cell transfer, and CD69-deficient mice that received unprimed WT CD4 T cells (unp. WT), OVA-primed WT CD4 T cells (OVAp.WT), unprimed CD69-deficient CD4 T cells (unp.KO), or OVA-primed CD69-deficient CD4 T cells (OVAp.KO). The absolute cell numbers of eosinophils (Eosino.), lymphocytes (Lympho.), neutrophils (Neutro.), and macrophages (Mac.) are shown with the SEM. Four mice from each group were used in this experiment. *, $p < 0.01$ and **, $p < 0.05$. *C*, The lung specimens were fixed and stained with Luna. The results of the peribronchiolar eosinophilic infiltrates are shown with the SEM. *, $p < 0.01$ and **, $p < 0.05$. *D*, OVA-induced AHR was induced as in Fig. 1. OVA-sensitized CD69-deficient mice received i.v. 1×10^7 CD4 T cells from unprimed (unp.) or OVA-primed (OVAp.) WT or CD69-deficient (KO) mice 1 day before the first airway challenge with aerosolized OVA. The level of AHR was monitored by measuring Penh. Mean values of the percent above baseline are shown with the SEM ($n = 4$). *, $p < 0.01$ and **, $p < 0.05$ (between WT/OVA, ■ and CD69KO/OVA, ●, and between KO/OVA + OVAp.WT CD4T, ▲, and KO/OVA + OVAp.KO CD4T; ♦). *E* and *F*, The AHR was also assessed by measuring RL (*E*) and Cdyn (*F*). Mean values of the percent changes above baseline are shown with the SEM ($n = 5$). *, $p < 0.01$ and **, $p < 0.05$ (between KO/OVA + OVAp.WT CD4T, ▲, and KO/OVA, ●). *G*, The lung specimens were fixed and stained with PAS. A representative staining pattern in each group is shown. Original magnification, ×200. *H*, The numerical scores of PAS-stained cells.

Downloaded from www.jimmunol.org on February 23, 2010

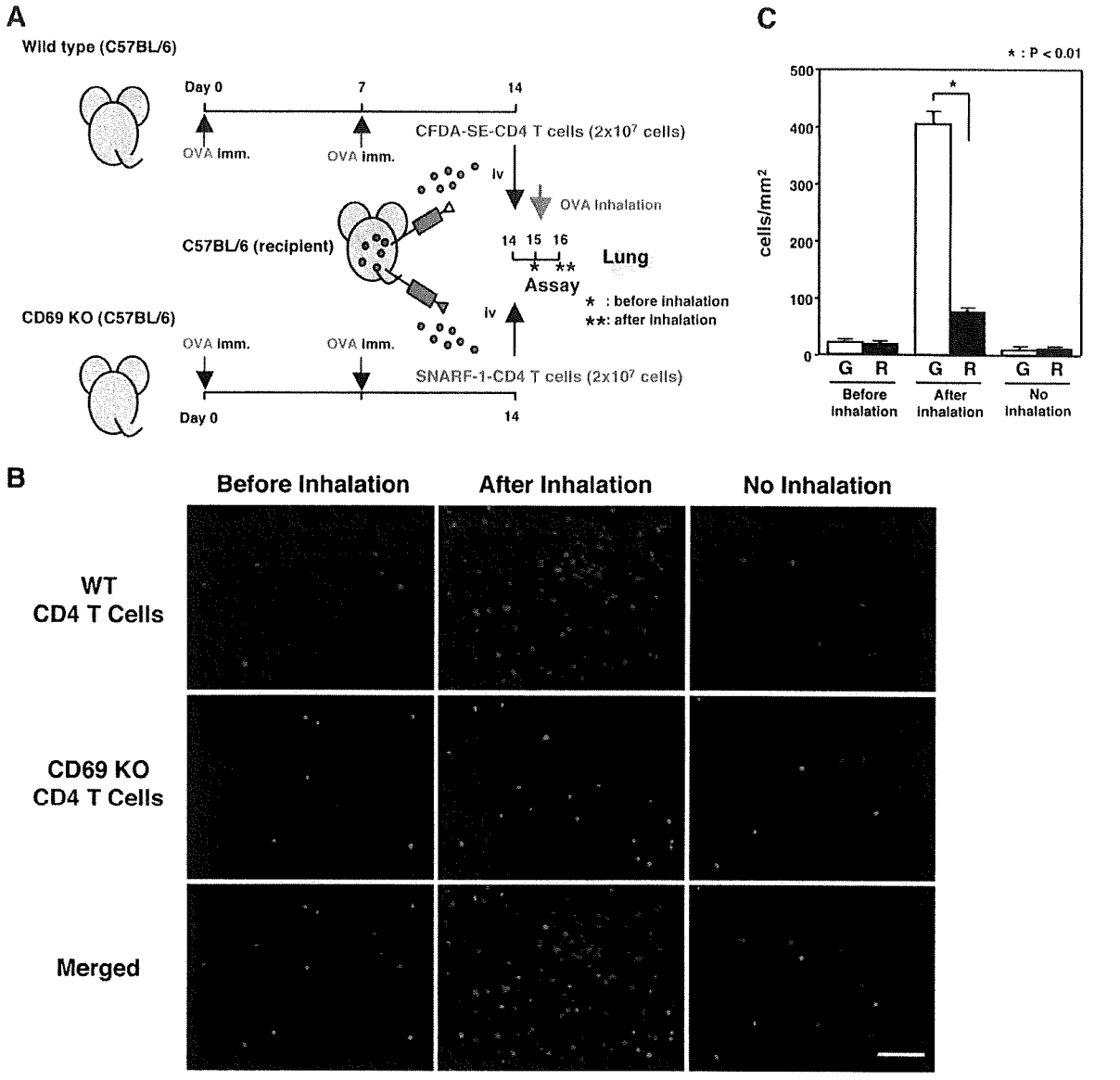

FIGURE 5. Color-coded fluorescence imaging of $CD4^+$ T cell infiltration into the lung during OVA-induced allergic asthma. *A*, A schematic overview of the study protocol for the induction of asthma. WT and CD69-deficient (CD69KO) mice were immunized with OVA on days 0 and 7. Splenic $CD4^+$ T cells were purified and labeled with either CFDA-SE (4 μM) or SNARF-1 (5 μM) at 37°C for 15 min. Twenty million CD4 T cells were injected i.v. into normal C57BL/6 mice on day 14. The recipient mice were exposed to airway challenge with aerosolized OVA on day 15. *B*, CFDA-SE- or SNARF-1-labeled CD4 T cells in the excised lungs were monitored before OVA inhalation on day 15 and 24 h after OVA inhalation on day 16 using the M205FA fluorescence microscope equipped with the VB-7010 CCD color camera system. Bar, 100 μm. *C*, Summary of the accumulation of fluorescent cells. Data are from 15 fields from three mice with the SD. □, Green fluorescent cells; ■, red fluorescent cells. *, $p < 0.01$ by Student's *t* test.

to monitor the green and red fluorescent T cells at the near surface area of the lung. As can be seen in Fig. 5, *B* and *C*, CFDA-SE-labeled green fluorescent cells from WT mice accumulated dramatically 1 day after inhalation. In contrast, the accumulation of the SNARF-1-labeled red fluorescent cells from CD69-deficient mice was marginal (Fig. 5*C*). Similar results were obtained when we used the opposite color-coded pattern for WT and CD69-deficient mice (data not shown). These results indicate that the migration of CD69-deficient CD4 T cells into the inflamed lung was impaired in comparison to that of WT CD4 T cells.

Reduced VCAM-1 induction and Th2 cell migration in the asthmatic lung of mice received CD69-deficient Th2 cells

VCAM-1 expression is induced in the asthmatic lung, and the VCAM-1/VLA-4 interaction is critical for the migration of T cells and the induction of Th2-dependent airway inflammation (32, 33). To test the involvement of VCAM-1 in the CD69-dependent airway inflammation, an immunofluorescent staining analysis with anti-VCAM-1 was performed. In vitro-generated WT and CD69-deficient DO11.10 Tg Th2 cells were transferred into unprimed BALB/c mice and the mice were exposed to OVA challenge with two cycles of inhalation (Fig. 6*A*). As expected, the induction of eosinophilic infiltration was dramatically impaired in the mice transferred with CD69-deficient Th2 cells accompanied with the decreased donor-derived $KJ1^+CD4^+$ Th2 cells in the lung (Fig. 6, *B* and *C*). The expression of VCAM-1, assessed by immunofluorescent staining analysis as seen in Fig. 6*D*, was substantially induced in the lung of mice with WT Th2 cell transfer, but it was marginal at best in the mice with CD69-deficient Th2 cell transfer. These

Downloaded from www.jimmunol.org on February 23, 2010

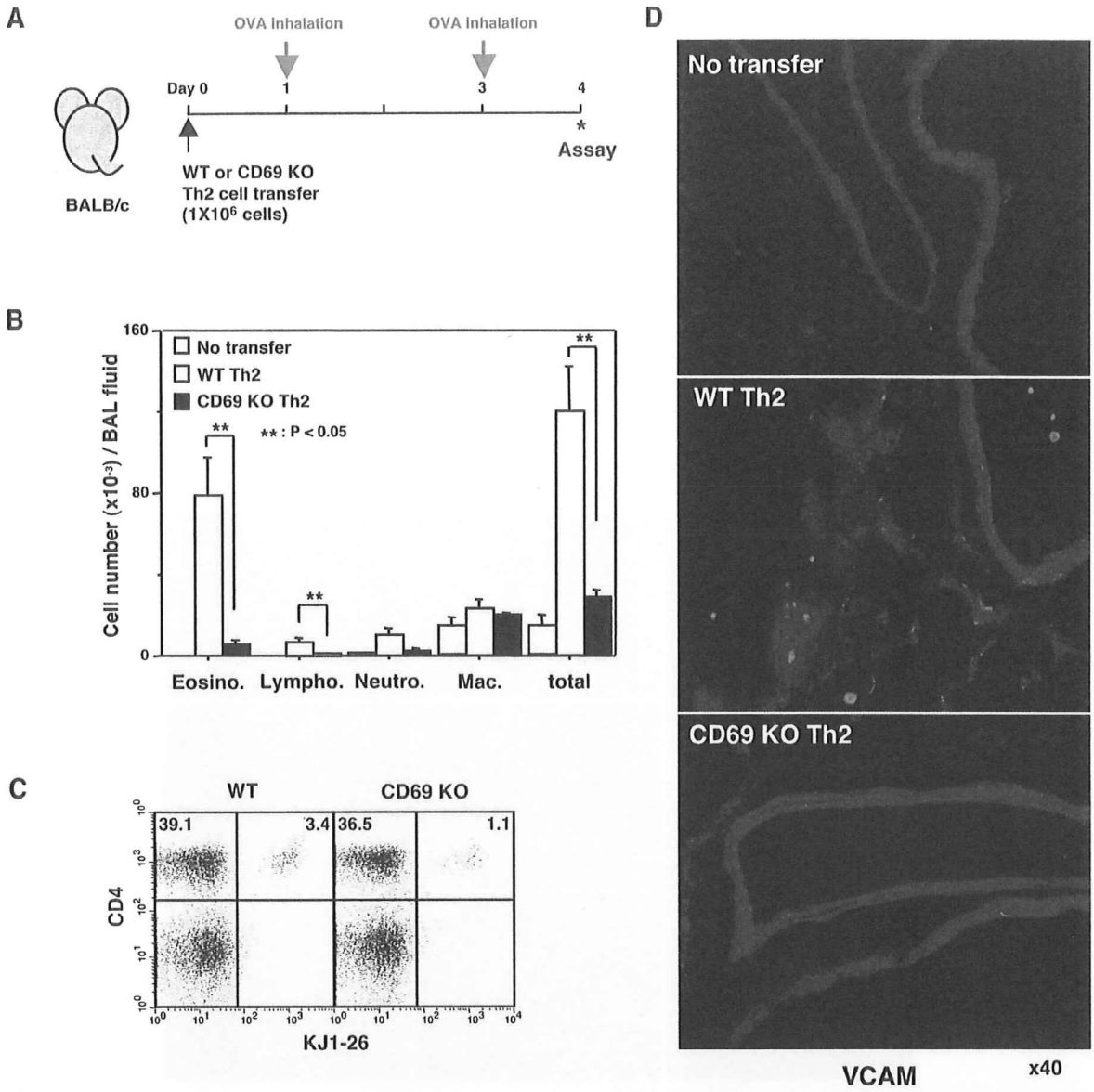

FIGURE 6. Reduced VCAM-1 induction and Th2 cell migration in the asthmatic lung of mice that received CD69-deficient Th2 cells. *A*, A schematic overview of the study protocol for the induction of asthma. OVA-specific DO11.10 Tg CD69-deficient Th2 cells (1×10^6) were transferred into BALB/c mice. The recipient mice were exposed to OVA challenges by inhalation 1 and 3 days after cell transfer. *B*, The cells in the BAL fluid from WT mice that did not receive cells (no transfer), WT mice that received WT Th2 cells (WT Th2), or CD69-deficient Th2 cells (CD69KO Th2) were analyzed. The absolute cell numbers of eosinophils (Eosino.), lymphocytes (Lympho.), neutrophils (Neutro.), and macrophages (Mac.) are shown with SDs. **, $p < 0.05$ (between WT transfer and CD69KO transfer). *C*, Representative CD4/KJ1-26 profiles of the lung leukocytes from the mice that received WT or CD69-deficient Th2 cells. *D*, Fluorescence microscopic analysis of the lung was performed using Abs for VCAM-1 (red). Blue represents the tissue autofluorescence.

results suggest that VCAM-1 is involved in the CD69-dependent migration of Th2 cells into the asthmatic lung.

In vivo treatment with anti-CD69 mAb inhibited the induction and the maintenance of OVA-induced airway inflammation and AHR

To explore the therapeutic effect of the administration of anti-CD69 mAb during allergic airway inflammation, WT BALB/c mice were immunized with OVA on days 0 and 7 and then treated with anti-CD69 mAb or control Ab 1 day before the first airway challenge with OVA (Fig. 7*A*). The examination of infiltrated cells in the BAL fluid revealed a marked decrease in the number of infiltrated eosinophils in the BAL fluid (Fig. 7*B*). Similarly, infiltrated eosinophils in the perivascular and peribronchiolar regions of the lung were lower in the mAb-treated animals (Fig. 7*C*). The treatment with anti-CD69 mAb resulted in a reduction of the extent of AHR (Fig. 7*D*) and milder mucus hyperproduction in the airways of mice treated with anti-CD69 mAb in comparison to the mice receiving control Abs (Fig. 7, *E* and *F*). These results suggest that the development of OVA-induced airway inflammation and AHR could be inhibited by treatment with anti-CD69 mAb.

Furthermore, when anti-CD69 mAb or control mAb was administered after the last OVA inhalation (on day 16), an examination of infiltration of inflammatory cells, including eosinophils and lymphocytes in the BAL fluid 1, 3, and 5 days after the last OVA inhalation (Fig. 7*G*), revealed that infiltration of inflammatory cells

Downloaded from www.jimmunol.org on February 23, 2010

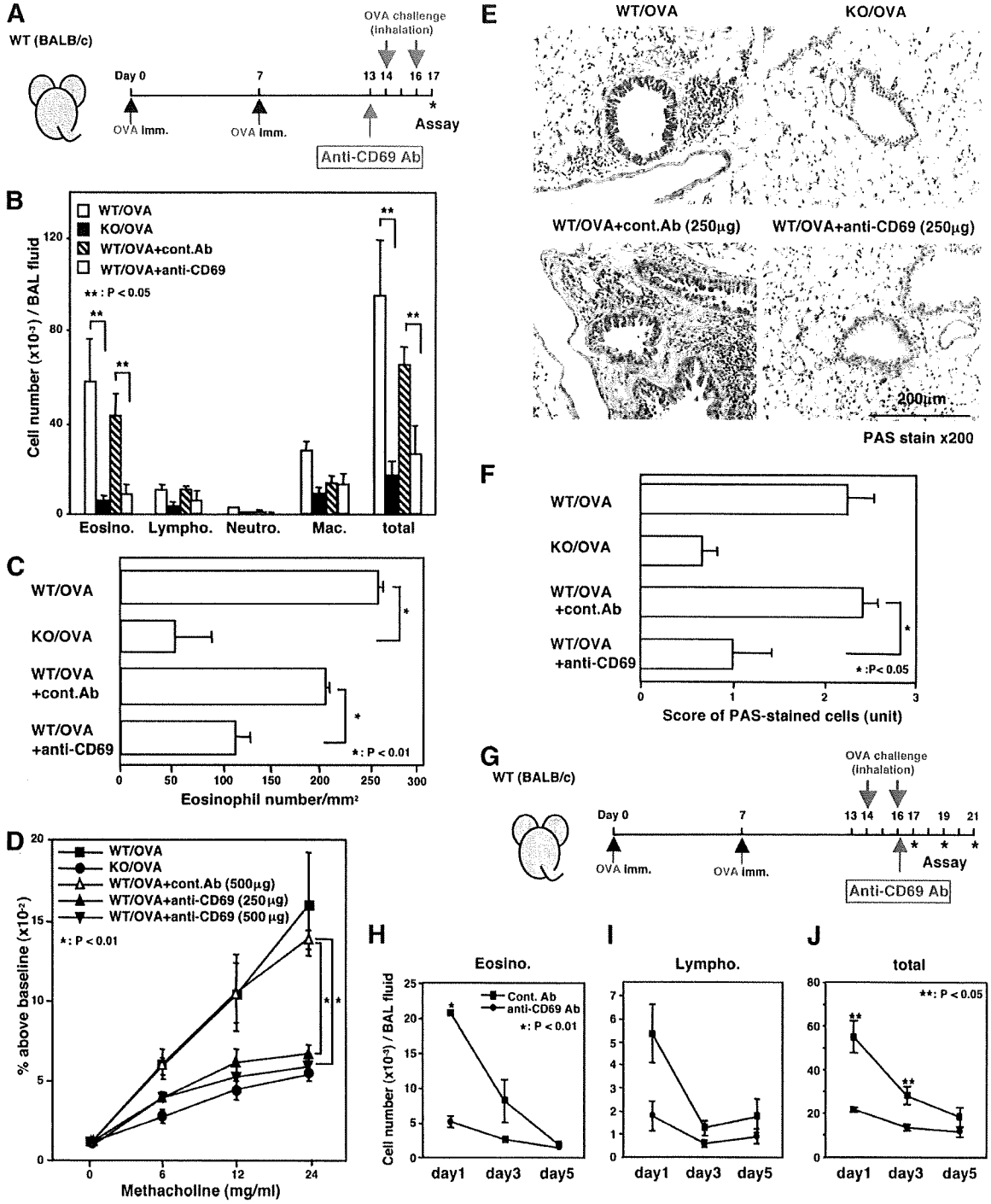

FIGURE 7. Effect of in vivo treatment with anti-CD69 mAb on OVA-induced airway inflammation and AHR. *A*, Six-week-old WT mice were sensitized with OVA-alum and were subsequently challenged with OVA on days 14 and 16. The mice were treated with anti-CD69 mAb or control hamster IgG 24 h before the first airway challenge with aerosolized OVA. *B*, WT BALB/c mice were treated with anti-CD69 mAb or control hamster IgG 24 h before the first airway challenge with aerosolized OVA. One day after the last challenge, the mice were sacrificed and the BAL fluid was collected. The absolute cell number of eosinophils (Eosino.), lymphocytes (Lympho.), neutrophils (Neutro.), and macrophages (Mac.) are shown with the SEM. Four mice from each group were used in this experiment. **, $p < 0.05$ (between WT/OVA and KO/OVA groups and between control Ab- (cont.Ab) and anti-CD69-treated groups). *C*, The lung specimens were fixed and stained with Luna. The results of peribronchiolar eosinophilic infiltrates are shown with SDs. *, $p < 0.01$. *D*, OVA-induced AHR was induced as in Fig. 1. WT BALB/c mice were treated with anti-CD69 mAb or control hamster IgG 24 h before the first airway challenge with aerosolized OVA. Mean values of the percent above baseline are shown with the SEM ($n = 4$). Five independent experiments were performed with similar results. *, $p < 0.01$ (between cont.Ab- and anti-CD69-treated groups). *E*, The lung specimens were fixed and stained with PAS. A representative staining pattern from each group is shown. Original magnification, ×200. *F*, The numerical scores of PAS-stained cells. *G*, The OVA-sensitized and challenged mice were treated with anti-CD69 mAb or control hamster IgG just after the last OVA inhalation, and the BAL fluid was collected on days 17, 19, and 21. *H–J*, Anti-CD69 mAb was administered just after the last OVA inhalation (on day 16) and the BAL fluid was collected 1, 3, and 5 days later. The numbers of infiltrated eosinophils (*H*), lymphocytes (*I*), and total leukocytes (*J*) are shown with the SEM (five mice in each group). *, $p < 0.01$ and **, $p < 0.05$.

Downloaded from www.jimmunol.org on February 23, 2010

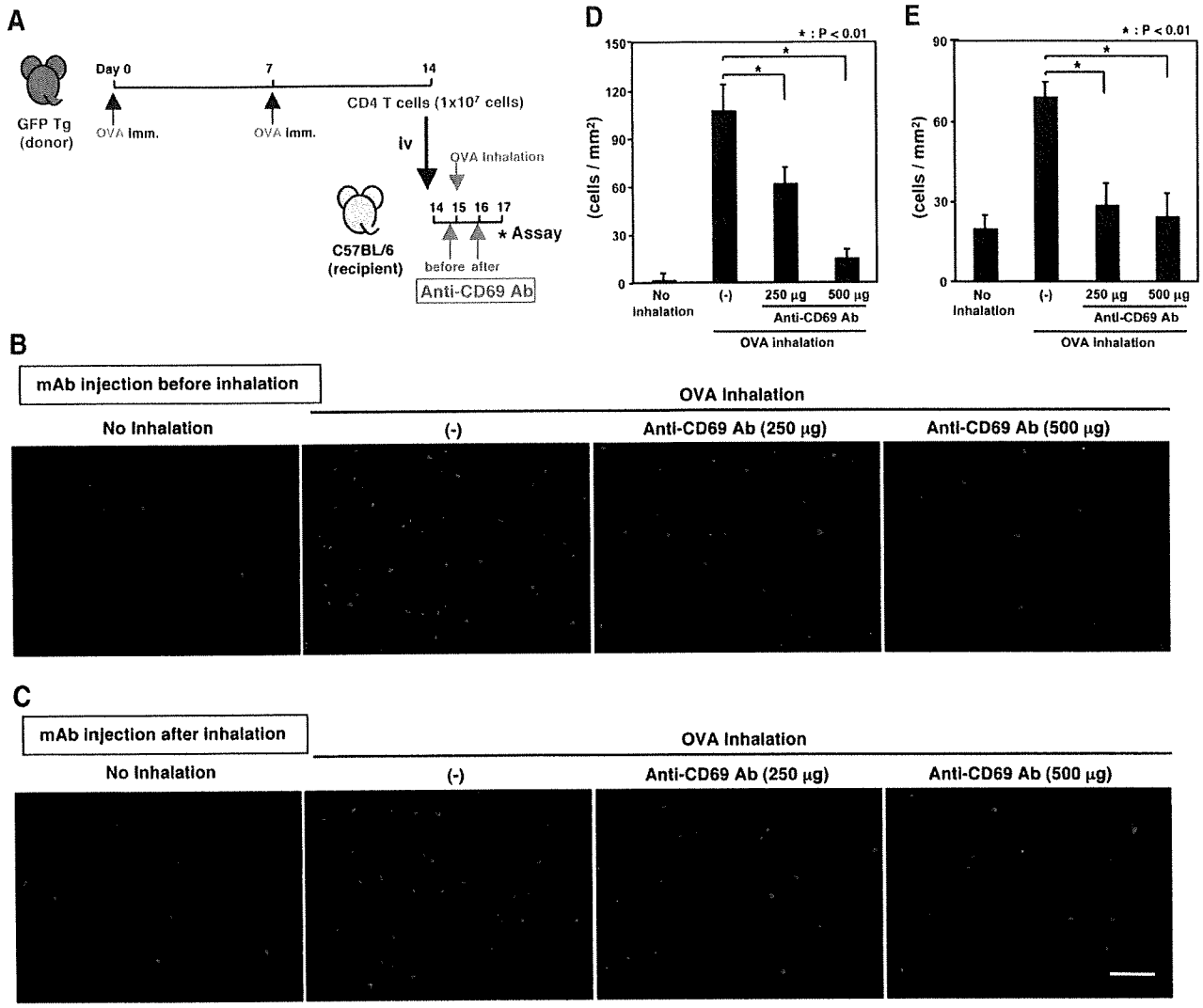

FIGURE 8. Effect of in vivo treatment with anti-CD69 mAb on CD4 T cell migration in the asthmatic lung. *A*, A schematic overview of the study protocol. GFP Tg mice were immunized with OVA on days 0 and 7. Splenic $CD4^+$ T cells (1×10^7) from OVA-sensitized GFP Tg mice were purified and injected into normal C57BL/6 mice on day 14. The recipient mice were exposed to airway challenge with aerosolized OVA on day 15. Anti-CD69 mAb (250 or 500 μg) was administered 1 h before OVA inhalation or 1 day after OVA inhalation. Mice were analyzed on day 17. *B* and *C*, Color-coded images of CD4 T cells. GFP^+ CD4 T cells in the excised lung were monitored 2 days after OVA inhalation on day 17 using the M205FA fluorescence microscope equipped with the VB-7010 CCD color camera system. Bar, 100 μm. *D* and *E*, The numbers represent the absolute cell number of CD4 T cells/mm^2 with SD, $n = 20$ fields). *, $p < 0.01$.

including eosinophils and lymphocytes decreased gradually in the control mAb-injected groups, whereas inflammatory cell infiltration was already substantially lower on day 1 in the groups receiving anti-CD69 mAb (Fig. 7, *H–J*). These results indicate that the recovery from airway inflammation occurred more quickly even when anti-CD69 mAb was administered after the onset of airway inflammation. Thus, a therapeutic effect of anti-CD69 mAb is suggested from this allergic asthma model.

In vivo treatment with anti-CD69 mAb inhibited the migration of OVA-primed Th2 cells

Finally, to evaluate the extent of CD4 T cell migration in the inflamed lung of mice treated with anti-CD69 mAb, GFP Tg mice with a C57BL/6 background were immunized on days 0 and 7 and then splenic CD4 T cells were transferred into normal C57BL/6 mice. One day after cell transfer, the mice were challenged with OVA by inhalation. Anti-CD69 mAb was injected 1 h before inhalation or 1 day after inhalation (Fig. 8*A*). As can be seen in Fig. 8, *B* and *D*, the migration of OVA-primed CD4 T cells was inhibited in a dose-dependent manner when the mice were treated with anti-CD69 mAb before inhalation. The migration of OVA-primed CD4 T cells tested on day 17 was also inhibited when the mice were treated with anti-CD69 mAb 1 day after inhalation (Fig. 8, *C* and *E*). These results indicate that the treatment with anti-CD69 mAb resulted in the inhibition of CD4 T cell migration in the inflamed lung, further supporting the therapeutic effect of anti-CD69 mAb treatment.

Discussion

Murine models of allergic airway inflammation have been used to dissect the underlying pathogenesis of asthma. In this study, we used an OVA-induced allergic asthma model and CD69-deficient mice to demonstrate that CD69 on CD4 Th2 cells

Downloaded from www.jimmunol.org on February 23, 2010

plays an important role in the development of Ag-induced Th2-driven eosinophilic airway inflammation and AHR (Fig. 3). The attenuated airway inflammation in CD69-deficient mice appeared to be due largely to the reduced migration of Th2 cells into the inflamed lung (Fig. 5). The involvement of VCAM-1 expression was suggested (Fig. 6). In addition, a therapeutic effect of the administration of anti-CD69 mAb was revealed (Figs. 7 and 8), indicating that CD69 could be a new target for mAb treatment of asthmatic patients.

The deficit in the effector Th2 cell differentiation and Th2 cytokine expression was modest in CD69-deficient CD4 T cells (Fig. 2, *D* and *E*). However, the expression of IL-5, IL-13, and eotaxin 2 in the CD69-deficient CD4 T cells in the BAL fluid was substantially reduced (Fig. 2*A*), and Th2 cytokine expression (IL-4, IL-5, and IL-13) in the lung CD4 T cells was very low compared with that of WT (Fig. 2*B*). Airway inflammation and AHR were attenuated substantially in the absence of CD69 on CD4 T cells (Figs. 3 and 4). Using an imaging system to detect migration of CD4 T cells in the lung, we found that the migration of CD69-deficient CD4 T cells was severely inhibited (Fig. 5). Thus, the alteration in the development of airway inflammation and AHR in CD69-deficient mice appears to be due mainly to the impaired migration of CD69-deficient Th2 cells into the inflamed lung.

It is known that the expression of VCAM-1 on endothelial cells is induced in the inflamed lung and that VCAM-1 expression is critical for the recruitment of allergen-specific T cells and eosinophils during allergic airway inflammation (32, 33). VCAM-1/VLA-4 interaction was shown to be important for the recruitment of T cells in the inflamed tissues (32). IL-13 has been recognized as a molecule that induces VCAM-1 expression in endothelial cells during allergic inflammation (5, 34). Several small molecule inhibitors of the interaction of VLA-4/VCAM-1 have been reported to attenuate allergic inflammation (35, 36). We detected a substantially reduced expression of IL-13 in the infiltrated CD4 T cells in the BAL fluid and the lung tissue in CD69-deficient mice (Fig. 2, *A* and *B*). Marginal induction of the expression of VCAM-1 in the lung of mice that received CD69-deficient Th2 cells was observed (Fig. 6). Thus, the effect on the migration of CD69-deficient Th2 cells appears to be at least in part due to the failure to induce VCAM-1 expression in the asthmatic lung. However, more precise molecular mechanisms underlying the CD69-dependent Th2 cell migration into the inflamed lung will require further investigation.

Although the ligand for CD69 has not been identified, a possible scenario is that a putative ligand may be induced and expressed on the inflamed lung tissues. Activated Th2 cells expressing CD69 then may migrate into the lung tissue and remain at the inflammatory site efficiently via the CD69/CD69 ligand interaction. CD69-deficient CD4 T cells, in contrast, may not be retained at the inflammatory site very efficiently because of the lack of this interaction.

The regulatory roles of CD69 in an anti-collagen Ab-induced arthritis model (16) and a collagen-induced arthritis model (15) have been reported. In an anti-collagen Ab-induced arthritis model, a critical role for CD69 in neutrophil function at the effector phase was indicated. In a collagen-induced arthritis model, it is suggested that CD69 is a negative regulator of arthritis through TGF-β synthesis during the induction phase. In our mouse model of OVA-induced asthma, the expression levels of TGF-β in the BAL fluid and in the activated spleen cells in vitro were similar between WT and CD69-deficient mice (T. Nakayama, unpublished observation). Therefore, the CD69-mediated induction of TGF-β synthesis appeared not to be involved in the regulation of Th2 cell differentiation and/or the regulation of Th2-driven allergic airway inflammation. Thus, CD69 can play different roles in the initiation of inflammatory immune responses. CD69 is also expressed on activated B cells. Although B cell development appeared to be mildly affected in CD69-deficient mice, normal proliferative responses of peripheral B cells were detected (37). We also observed normal IgG1 and IgE production in CD69-deficient B cell cultures after LPS and IL-4 stimulation (T. Nakayama, unpublished observation). Thus, the function of B cells appeared to be less dependent on CD69, suggesting a redundant mechanism during B cell activation.

It was recently reported that CD69 is physically associated with spingosine 1-phosphate receptor 1 ($S1P_1$) and inhibits the S1P/$S1P_1$-mediated egress of the cells from the lymphoid organs (17). To address the involvement of $S1P_1$-mediated regulation of CD4 T cell egress in the CD69-dependent airway inflammation, we used FTY720, which acts on $S1P_1$ to inhibit the egress of lymphocytes from the lymph nodes. The numbers of CD4 and CD8 T cells in the peripheral blood, spleen, and lymph nodes were equivalent between WT and CD69-deficient mice even after OVA immunization and challenge, and their numbers in the peripheral blood were reduced equivalently when FTY720 was administered (T. Nakayama unpublished observation). We observed reduced airway inflammation and AHR in CD69-deficient mice (Fig. 1). Although FTY720 injection reduced the extent of OVA-induced eosinophilic airway inflammation and AHR in WT mice, no effect was observed in CD69-deficient mice (T. Nakayama unpublished observation). Moreover, CD69-mediated inhibition of $S1P_1$ function appeared to be observed only when CD69 up-regulation is induced with IFN-α/β (17). No significant amount of IFN-α/β was detected in the BAL fluid in our OVA-induced airway inflammation model (T. Nakayama, unpublished observation). Thus, in our allergic airway inflammation model, S1P/$S1P_1$-mediated regulation of lymphocyte egress from the lymph nodes does not appear to account for the change in the airway inflammation induced by CD69-deficient Th2 cells.

We used an imaging system to follow Th2 cell migration into the lung with a fluorescent microscope and CD4 T cells labeled with a fluorescent dye (Fig. 5) or GFP Tg T cells (Fig. 8). We detected infiltrated CD4 T cells at the near surface area of the asthmatic lung. Migration of CD4 T cells into the parenchyma or through the endothelial cells of the lung vessels has been reported (33). The imaging system used here is useful for the quantitative detection of the migrated lymphocytes into the asthmatic lung, since the number of lymphocytes including Th2 cells is relatively small among inflammatory cells such as eosinophils.

In a model of Th1-induced airway inflammation characterized by the neutrophilic infiltration, CD69-deficient Th1 cells also showed reduced levels of airway inflammation compared with WT (T. Nakayama, unpublished observation). Although the molecular and cellular mechanisms involved in the Th1-induced airway inflammation is distinct from that of Th2-cell induced eosinophilic inflammation, this result indicates that CD69 on Th1 cells also plays an important role in the induction of airway inflammation.

This study demonstrated the therapeutic effect of the administration of anti-CD69 mAb (Figs. 7 and 8). The anti-CD69 Ab treatment via the airway also showed a significant inhibitory effect (our unpublished observation). The ligand for CD69 has not been identified, but it is possible that anti-CD69 mAb blocks the interaction of CD69 and putative CD69 ligands, resulting in the reduced Th2 cell migration and attenuated airway inflammation. Although a very early study suggested that the anti-CD69 mAb if cross-linked induced the enhancement of Con A-induced proliferation of T cells in vitro (38), we have not detected any dramatic effect on T cell numbers or the phenotypes of CD4 T cells in the lung or spleen of

Downloaded from www.jimmunol.org on February 23, 2010

mice receiving anti-CD69 mAb (T. Nakayama unpublished observation). In any event, it is notable that a potent therapeutic effect of the anti-CD69 mAb administration was observed even after the onset of airway inflammation.

In summary, our results indicate that CD69 on CD4 T cells plays a critical role in the development of allergen-induced eosinophilic inflammation and AHR by effecting efficient migration of activated Th2 cells into the asthmatic lung. Moreover, our mAb administration experiments revealed that CD69 could consequently be a possible therapeutic target for the treatment of asthmatic patients.

Acknowledgments

We are grateful to Dr. Ralph T. Kubo for helpful comments and constructive criticisms in the preparation of this manuscript. We thank Kaoru Sugaya, Hikari Asou, Satoko Norikane, and Toshihiro Ito for excellent technical assistance.

Disclosures

The authors have no financial conflict of interest.

References

1. McFadden, E. R., Jr., and I. A. Gilbert. 1992. Asthma. *N. Engl. J. Med.* 327: 1928–1937.
2. Busse, W. W., and R. F. Lemanske, Jr. 2001. Asthma. *N. Engl. J. Med.* 344: 350–362.
3. Hamelmann, E., and E. W. Gelfand. 2001. IL-5-induced airway eosinophilia–the key to asthma? *Immunol. Rev.* 179: 182–191.
4. Lloyd, C. M., J. A. Gonzalo, A. J. Coyle, and J. C. Gutierrez-Ramos. 2001. Mouse models of allergic airway disease. *Adv. Immunol.* 77: 263–295.
5. Wills-Karp, M. 2004. Interleukin-13 in asthma pathogenesis. *Immunol. Rev.* 202: 175–190.
6. Cohn, L., J. A. Elias, and G. L. Chupp. 2004. Asthma: mechanisms of disease persistence and progression. *Annu. Rev. Immunol.* 22: 789–815.
7. Umetsu, D. T., and R. H. DeKruyff. 2006. The regulation of allergy and asthma. *Immunol. Rev.* 212: 238–255.
8. Robinson, D. S., Q. Hamid, S. Ying, A. Tsicopoulos, J. Barkans, A. M. Bentley, C. Corrigan, S. R. Durham, and A. B. Kay. 1992. Predominant TH2-like bronchoalveolar T-lymphocyte population in atopic asthma. *N. Engl. J. Med.* 326: 298–304.
9. Corrigan, C. J., Q. Hamid, J. North, J. Barkans, R. Moqbel, S. Durham, V. Gemou-Engesaeth, and A. B. Kay. 1995. Peripheral blood CD4 but not CD8 T-lymphocytes in patients with exacerbation of asthma transcribe and translate messenger RNA encoding cytokines which prolong eosinophil survival in the context of a Th2-type pattern: effect of glucocorticoid therapy. *Am. J. Respir. Cell Mol. Biol.* 12: 567–578.
10. Ziegler, S. F., F. Ramsdell, K. A. Hjerrild, R. J. Armitage, K. H. Grabstein, K. B. Hennen, T. Farrah, W. C. Fanslow, E. M. Shevach, and M. R. Alderson. 1993. Molecular characterization of the early activation antigen CD69: a type II membrane glycoprotein related to a family of natural killer cell activation antigens. *Eur. J. Immunol.* 23: 1643–1648.
11. Testi, R., D. D'Ambrosio, R. De Maria, and A. Santoni. 1994. The CD69 receptor: a multipurpose cell-surface trigger for hematopoietic cells. *Immunol. Today* 15: 479–483.
12. Sancho, D., M. Gomez, and F. Sanchez-Madrid. 2005. CD69 is an immunoregulatory molecule induced following activation. *Trends Immunol.* 26: 136–140.
13. Nakayama, T., D. J. Kasprowicz, M. Yamashita, L. A. Schubert, G. Gillard, M. Kimura, A. Didierlaurent, H. Koseki, and S. F. Ziegler. 2002. The generation of mature, single-positive thymocytes in vivo is dysregulated by CD69 blockade or overexpression. *J. Immunol.* 168: 87–94.
14. Feng, C., K. J. Woodside, B. A. Vance, D. El-Khoury, M. Canelles, J. Lee, R. Gress, B. J. Fowlkes, E. W. Shores, and P. E. Love. 2002. A potential role for CD69 in thymocyte emigration. *Int. Immunol.* 14: 535–544.
15. Sancho, D., M. Gomez, F. Viedma, E. Esplugues, M. Gordon-Alonso, M. A. Garcia-Lopez, H. de la Fuente, A. C. Martinez, P. Lauzurica, and F. Sanchez-Madrid. 2003. CD69 downregulates autoimmune reactivity through active transforming growth factor-β production in collagen-induced arthritis. *J. Clin. Invest.* 112: 872–882.
16. Murata, K., M. Inami, A. Hasegawa, S. Kubo, M. Kimura, M. Yamashita, H. Hosokawa, T. Nagao, K. Suzuki, K. Hashimoto, et al. 2003. CD69-null mice protected from arthritis induced with anti-type II collagen antibodies. *Int. Immunol.* 15: 987–992.
17. Shiow, L. R., D. B. Rosen, N. Brdickova, Y. Xu, J. An, L. L. Lanier, J. G. Cyster, and M. Matloubian. 2006. CD69 acts downstream of interferon-α/β to inhibit $S1P_1$ and lymphocyte egress from lymphoid organs. *Nature* 440: 540–544.
18. Okabe, M., M. Ikawa, K. Kominami, T. Nakanishi, and Y. Nishimune. 1997. "Green mice" as a source of ubiquitous green cells. *Federation Eur. Biochem. Soc. Lett.* 407: 313–319.
19. Murphy, K. M., A. B. Heimberger, and D. Y. Loh. 1990. Induction by antigen of intrathymic apoptosis of $CD4^+CD8^+TCR^{low}$ thymocytes in vivo. *Science* 250: 1720–1723.
20. Nakayama, T., C. H. June, T. I. Munitz, M. Sheard, S. A. McCarthy, S. O. Sharrow, L. E. Samelson, and A. Singer. 1990. Inhibition of T cell receptor expression and function in immature $CD4^+CD8^+$ cells by CD4. *Science* 249: 1558–1561.
21. Yamashita, M., M. Kimura, M. Kubo, C. Shimizu, T. Tada, R. M. Perlmutter, and T. Nakayama. 1999. T cell antigen receptor-mediated activation of the Ras/mitogen- activated protein kinase pathway controls interleukin 4 receptor function and type-2 helper T cell differentiation. *Proc. Natl. Acad. Sci. USA* 96: 1024–1029.
22. Kamata, T., M. Yamashita, M. Kimura, K. Murata, M. Inami, C. Shimizu, K. Sugaya, C. R. Wang, M. Taniguchi, and T. Nakayama. 2003. *src* homology 2 domain-containing tyrosine phosphatase SHP-1 controls the development of allergic airway inflammation. *J. Clin. Invest.* 111: 109–119.
23. Myou, S., A. R. Leff, S. Myo, E. Boetticher, J. Tong, A. Y. Meliton, J. Liu, N. M. Munoz, and X. Zhu. 2003. Blockade of inflammation and airway hyperresponsiveness in immune-sensitized mice by dominant-negative phosphoinositide 3-kinase-TAT. *J. Exp. Med.* 198: 1573–1582.
24. Nigo, Y. I., M. Yamashita, K. Hirahara, R. Shinnakasu, M. Inami, M. Kimura, A. Hasegawa, Y. Kohno, and T. Nakayama. 2006. Regulation of allergic airway inflammation through Toll-like receptor 4-mediated modification of mast cell function. *Proc. Natl. Acad. Sci. USA* 103: 2286–2291.
25. Kimura, M. Y., H. Hosokawa, M. Yamashita, A. Hasegawa, C. Iwamura, H. Watarai, M. Taniguchi, T. Takagi, S. Ishii, and T. Nakayama. 2005. Regulation of T helper type 2 cell differentiation by murine Schnurri-2. *J. Exp. Med.* 201: 397–408.
26. Kang, H. S., S. E. Blink, R. K. Chin, Y. Lee, O. Kim, J. Weinstock, T. Waldschmidt, D. Conrad, B. Chen, J. Solway, A. I. Sperling, and Y. X. Fu. 2003. Lymphotoxin is required for maintaining physiological levels of serum IgE that minimizes Th1-mediated airway inflammation. *J. Exp. Med.* 198: 1643–1652.
27. Koya, T., T. Kodama, K. Takeda, N. Miyahara, E. S. Yang, C. Taube, A. Joetham, J. W. Park, A. Dakhama, and E. W. Gelfand. 2006. Importance of myeloid dendritic cells in persistent airway disease after repeated allergen exposure. *Am. J. Respir Crit. Care Med.* 173: 42–55.
28. Hirahara, K., M. Yamashita, C. Iwamura, K. Shinoda, A. Hasegawa, H. Yoshizawa, H. Koseki, F. Gejyo, and T. Nakayama. 2008. 2008. Repressor of GATA regulates T_H2-driven allergic airway inflammation and airway hyperresponsiveness. *J. Allergy Clin. Immunol.* 122: 512–520.
29. Kimura, M., Y. Koseki, M. Yamashita, N. Watanabe, C. Shimizu, T. Katsumoto, T. Kitamura, M. Taniguchi, H. Koseki, and T. Nakayama. 2001. Regulation of Th2 cell differentiation by *mel-18*, a mammalian *polycomb* group gene. *Immunity* 15: 275–287.
30. Hasegawa, A., K. Hayashi, H. Kishimoto, M. Yang, S. Tofukuji, K. Suzuki, H. Nakajima, R. M. Hoffman, M. Shirai, and T. Nakayama. 2009. Color-coded real-time cellular imaging of T lymphocyte accumulation and focus formation in mouse asthma model. *J. Allergy Clin. Immunol.* In press.
31. Wands, J. M., C. L. Roark, M. K. Aydintug, N. Jin, Y. S. Hahn, L. Cook, X. Yin, J. Dal Porto, M. Lahn, D. M. Hyde, Born, et al. 2005. Distribution and leukocyte contacts of $\gamma\delta$ T cells in the lung. *J. Leukocyte Biol.* 78: 1086–1096.
32. Nakajima, H., H. Sano, T. Nishimura, S. Yoshida, and I. Iwamoto. 1994. Role of vascular cell adhesion molecule 1/very late activation antigen 4 and intercellular adhesion molecule 1/lymphocyte function-associated antigen 1 interactions in antigen-induced eosinophil and T cell recruitment into the tissue. *J. Exp. Med.* 179: 1145–1154.
33. Kaminuma, O., H. Fujimura, K. Fushimi, A. Nakata, A. Sakai, S. Chishima, K. Ogawa, M. Kikuchi, H. Kikkawa, K. Akiyama, and A. Mori. 2001. Dynamics of antigen-specific helper T cells at the initiation of airway eosinophilic inflammation. *Eur. J. Immunol.* 31: 2669–2679.
34. Bochner, B. S., D. A. Klunk, S. A. Sterbinsky, R. L. Coffman, and R. P. Schleimer. 1995. IL-13 selectively induces vascular cell adhesion molecule-1 expression in human endothelial cells. *J. Immunol.* 154: 799–803.
35. Sedgwick, J. B., K. J. Jansen, J. D. Kennedy, H. Kita, and W. W. Busse. 2005. Effects of the very late adhesion molecule 4 antagonist WAY103 on human peripheral blood eosinophil vascular cell adhesion molecule 1-dependent functions. *J. Allergy Clin. Immunol.* 116: 812–819.
36. Okigami, H., K. Takeshita, M. Tajimi, H. Komura, M. Albers, T. E. Lehmann, T. Rolle, and K. B. Bacon. 2007. Inhibition of eosinophilia in vivo by a small molecule inhibitor of very late antigen (VLA)-4. *Eur. J. Pharmacol.* 559: 202–209.
37. Lauzurica, P., D. Sancho, M. Torres, B. Albella, M. Marazuela, T. Merino, J. A. Bueren, A. C. Martinez, and F. Sanchez-Madrid. 2000. Phenotypic and functional characteristics of hematopoietic cell lineages in CD69-deficient mice. *Blood* 95: 2312–2320.
38. Yokoyama, W. M., F. Koning, P. J. Kehn, G. M. Pereira, G. Stingl, J. E. Coligan, and E. M. Shevach. 1988. Characterization of a cell surface-expressed disulfide-linked dimer involved in murine T cell activation. *J. Immunol.* 141: 369–376.

Downloaded from www.jimmunol.org on February 23, 2010

Color-coded real-time cellular imaging of lung T-lymphocyte accumulation and focus formation in a mouse asthma model

Akihiro Hasegawa, PhD,[a,c,d] Katsuhiro Hayashi, MD,[d] Hiroyuki Kishimoto, MD, PhD,[d] Meng Yang, MD, PhD,[d] Soichi Tofukuji, MS,[a] Kazuo Suzuki, PhD,[a] Hiroshi Nakajima, MD, PhD,[b] Robert M. Hoffman, PhD,[d,e] Mutsunori Shirai, MD, PhD,[c] and Toshinori Nakayama, MD, PhD[a] *Chiba and Ube, Japan, and San Diego, Calif*

Background: A critical role for $CD4^+T_H2$ cells in the pathogenesis of acute asthma has been demonstrated in the studies of human asthma as well as of animal models of asthma. T_H2-cell migration into the lung is crucial for the initiation of asthma phenotype, but the dynamics of this process are poorly understood because it has been difficult to visualize this process.

Objective: Our aim was to image the cellular dynamics of the migration of T_H2 cells into the lung of living animals in a mouse model of asthma and identify the cellular processes required for the initiation of the asthma phenotype.

Methods: We developed a color-coded real-time imaging model of cell migration into the lung using green fluorescent protein (GFP) and red fluorescent protein (RFP) transgenic CD4 T cells.

Results: Selective accumulation of antigen-specific CD4 T cells in the lungs was quantitatively imaged in a mouse model of asthma. The inhibition of accumulation by dexamethasone was imaged. Accumulating GFP^+ T_H2 cells formed foci in the lungs from 6 to 20 hours after antigen inhalation. This process was also inhibited by the administration of anti–intercellular adhesion molecule 1 or anti–vascular cell adhesion molecule 1 mAbs. Two days after inhalation of antigen, GFP^+ T_H2 cells were detected in the area of eosinophil infiltration.

Conclusion: Focus formation generated by accumulating antigen-specific T_H2 cells in the lung appeared to be a critical process in the initiation of the asthma phenotype. This new model enables the study of *in vivo* cell biology of airway inflammation and novel drug discovery for lung inflammatory diseases. (J Allergy Clin Immunol 2010;125:461-8.)

Key words: *Real-time in vivo cellular imaging, cellular dynamics, T_H2 cells, mouse model of asthma, focus formation, airway inflammation, GFP, ICAM-1, VCAM-1*

Abbreviations used
DEX: Dexamethasone
GFP: Green fluorescent protein
H&E: Hematoxylin and eosin
ICAM-1: Intercellular adhesion molecule 1
NIH: National Institutes of Health
RFP: Red fluorescent protein
TCR: T-cell receptor
Tg: Transgenic
VCAM-1: Vascular cell adhesion molecule 1

Lung inflammatory diseases such as asthma are major public health problems that have increased markedly in prevalence in the past 3 decades.[1] Asthma is characterized by a chronic inflammatory disease of the lower airways that causes airway hyperresponsiveness to a wide variety of specific and nonspecific stimuli.[2,3] The cardinal features of acute asthma are airway inflammation predominated by eosinophils, hypersecretion of mucus, and airway hyperresponsiveness. A critical role for $CD4^+$ T_H2 cells in the pathogenesis of acute asthma has been demonstrated in studies of human asthma as well as in animal models of allergic airway inflammation.[4-10] Previous investigations have studied T-cell migration during allergic reactions by using an adoptive cell transfer system.[11-13] The administration of anti–intercellular adhesion molecule 1 (ICAM-1) or anti–vascular cell adhesion molecule 1 (VCAM-1) antibody resulted in the inhibition of eosinophilic airway inflammation.[14] However, the *in vivo* dynamics of cell migration into the lung during inflammation in living animals is poorly understood because of the lack of an appropriate *in vivo* cellular imaging model. The use of fluorescent proteins for imaging, which we pioneered, allowed us to monitor cell migration *in vivo*.[15] Green fluorescent protein (GFP) and red fluorescent protein (RFP) were used to label living cells genetically *in vivo* as well as *in vitro*[16,17] and served as a powerful tool to monitor the migration of specific lymphocytes in live animals.

We report here a novel *in vivo* real-time color-coded cellular imaging model to visualize the dynamics of migration of T cells in a mouse model of asthma. We have found that accumulating T_H2 cells formed foci in the lungs 6 to 20 hours after allergen inhalation. Focus formation was dependent on ICAM-1 and VCAM-1 and appeared to determine the site of eosinophilic infiltration, indicating that T_H2-cell focus formation is a critical process during the initiation of airway inflammation in this animal model.

METHODS

Mice

C57BL/6 were purchased from Charles River Laboratories (Wilmington, MA). C57BL/6-transgenic (Tg) (CAG-EGFP)C14-Y01-FM131Osb (GFP Tg, C57BL/6 background) mice expressed an enhanced GFP in all tissue under the

From the Departments of [a]Immunology and [b]Molecular Genetics, Graduate School of Medicine, Chiba University; [c]the Department of Microbiology and Immunology, Yamaguchi University School of Medicine; [d]AntiCancer, Inc, San Diego; and [e]the Department of Surgery, University of California San Diego.

Supported in part by the Global Center of Excellence (COE) Program (Global Center for Education and Research in Immune System Regulation and Treatment), Monbukagakusho (MEXT), Japan, and grants from the Ministry of Education, Culture, Sports, Science and Technology (Japan).

Disclosure of potential conflict of interest: The authors have declared that they have no conflict of interest.

Received for publication April 15, 2009; revised July 26, 2009; accepted for publication August 2, 2009.

Available online December 25, 2009.

Reprint requests: Toshinori Nakayama, MD, PhD, Department of Immunology (H3), Graduate School of Medicine, Chiba University, 1-8-1 Inohana, Chuo-ku, Chiba, 260-8670 Japan. E-mail: tnakayama@faculty.chiba-u.jp.

0091-6749/$36.00

© 2010 American Academy of Allergy, Asthma & Immunology

doi:10.1016/j.jaci.2009.09.016

control of the β-actin promoter.[16] C57BL/6 background RFP Tg mice expressed RFP (DsRed-2) under the control of the chicken β-actin promoter and cytomegalovirus enhancer.[17,18] Ovalbumin-specific T-cell receptor αβ transgenic (OT II Tg) mice[19] were maintained under specific pathogen-free conditions. All animal care was carried out in accordance with the National Institutes of Health (NIH) guidelines (NIH assurance no. A3873-01) at AntiCancer, Inc, and the guidelines of Chiba University. All animal experiments were performed at AntiCancer Inc.

In vitro T_H2-cell differentiation cultures

Green fluorescent protein Tg x OT II Tg $CD44^{low}$ CD4 T cells (2×10^5) were purified by cell sorting and stimulated with antigenic ovalbumin peptide (Loh 15, 1 μmol/L) and irradiated (30 Gy) syngeneic antigen-presenting cells (1×10^6) in the presence of exogenous IL-4 as described previously.[20]

Ovalbumin sensitization, cell transfer, and ovalbumin inhalation

The GFP or RFP Tg mice were immunized intraperitoneally with 250 μg ovalbumin (chicken egg albumin from Sigma St Louis, Mo) in 4 mg aluminum hydroxide gel (alum) on days 0 and 7. Splenic CD4 T cells from ovalbumin-sensitized GFP or RFP Tg mice were isolated by magnetic negative selection using a $CD4^+$ T-cell isolation kit (Miltenyi Biotec, Bergish Gladbach, Germany) on day 14, yielding a purity of >98%. These cells (2×10^7 cells) or ovalbumin-specific T_H2 cells (5×10^6 cells) were transferred intravenously through the tail vain to 8-week-old C57BL/6 recipient mice. One or 2 days later, the recipient mice inhaled aerosolized ovalbumin in saline (10 mg/mL) for 30 minutes with a supersonic nebulizer (NE-U07; Omron Co, Kyoto, Japan) as described previously.[21]

Fluorescence imaging of cell accumulation in the lung

The mice were killed by CO_2 asphyxiation at various times after ovalbumin inhalation. The lungs were removed, and GFP^+ cells that had accumulated in the excised lung were monitored by using an OV100 Small Animal Imaging System (Olympus Corp., Tokyo, Japan).[15,22,23]

Dexamethasone treatment

Splenic CD4 T cells (2×10^7 cells) were transferred intravenously through the tail vein to 8-week-old C57BL/6 recipient mice on day 14. One hour before the airway challenge by ovalbumin inhalation (on day 15), mice were injected intraperitoneally with dexamethasone (0.4, 1, or 4 mg/kg). The mice were exposed to allergen challenges on days 15, and transferred GFP^+ CD4 T cells were monitored on day 16. Where indicated, dexamethasone was injected 1 hour before (day 15) or 1 day after ovalbumin inhalation (day 16). Two days after OVA inhalation (day 17), GFP^+ CD4 T cells were monitored by using the OV100 Small Animal Imaging System.

Anti–ICAM-1 and anti–VCAM-1 antibody treatment

Ovalbumin-specific T_H2 cells (5×10^6 cells) were transferred intravenously through the tail vein of 8-week-old C57BL/6 recipient mice. Twenty-four hours before the airway challenge by ovalbumin inhalation, mice were injected intraperitoneally with 200 μg anti–ICAM-1 (YN1/1.7.4) or anti–VCAM-1 (429) mAbs.[14] One day after ovalbumin inhalation, transferred ovalbumin-specific T_H2 cells were monitored by using the OV100 Small Animal Imaging System.

In vivo imaging of lung infiltrating T cells by scanning laser microscopy

Control mice and mice given ovalbumin were prepared surgically at various indicated time points after ovalbumin administration for lung imaging. The mice were anesthetized and tracheostomized on the surgical bed and kept at 37°C. The right bronchus was clamped to stop movement during ventilation. The left lung was mechanically ventilated with O_2 at the normal respiratory rate to keep the mice alive. The clamped right lung was monitored with the IV100 scanning laser microscope (Olympus Corp., Tokyo, Japan). The IV100 microscope enabled imaging up to 100 μm depth from the surface of the lung. A 488-nm argon laser was used. To create an *in vivo* video image, images were recorded at 5-second intervals for 40 minutes. A focus was scored when more than 50% of the 2-dimentional area was occupied by the infiltrating GFP^+ cells. Crawling (motile) cells in the lung were defined as those that migrated or elongated to more than 50% of their diameter. The NIH Image software program (NIH Image J 1.41) was used for image analysis.

Lung histology and immunohistochemistry

The mice were killed by CO_2 asphyxiation at the indicated times after ovalbumin inhalation, and the lungs were infused with 10% (vol/vol) formalin in PBS or 4% (vol/vol) paraformaldehyde for fixation. The lung samples were sectioned, stained with hematoxylin and eosin (H&E), and examined for pathological changes under a light microscope at magnification ×50 or ×200.[7] Lung specimens were embedded in Tissue-Tek optimal cutting temperature compound (Sakura Fluelek, Tokyo, Japan), frozen in liquid nitrogen, and cut with a cryostat into 6-μm-thick sections. Endogenous peroxidase activity as well as nonspecific protein binding was sequentially blocked by using 0.6% hydrogen peroxide and Biotin-Blocking System reagent (DAKO, Glostrup, Denmark), respectively. The sections were incubated with hamster anti-GFP mAb (AdD Serotec, Oxford, UK) at 10 μg/mL overnight at 4°C and then were washed in TRIS-buffered saline with Tween. Bound antibody was detected by sequential incubation with biotinylated rabbit antihamster IgG and streptavidin–horseradish peroxidase followed by 3,3-diaminobenzidine (DAKOCytomation). The slides were then washed and counterstained with hematoxylin.

Statistical analysis

Experimental data were expressed as the means + SDs. The significance between 2 groups was determined by the 2-tailed Student *t* test.

RESULTS

Color-coded fluorescence imaging of selective accumulation of ovalbumin-primed CD4 T cells into the lung in an ovalbumin-induced acute-asthma mouse model

To examine the CD4 T-cell behavior in the lung of living mice in a mouse model of asthma, we developed a color-coded imaging model using GFP or RFP Tg CD4 T cells (Fig 1, *A*). Immediately after cell transfer, numerous transferred cells temporally and nonspecifically accumulated in the lung capillaries (data not shown). One day later, some of the cells remained in the lung with no significant difference between sensitized GFP^+ and non-sensitized RFP^+ cells (Fig 1, *B, left*; before inhalation). One day after ovalbumin inhalation, the number of GFP^+ CD4 T cells from ovalbumin-immunized mice increased significantly, and some of them formed foci (Fig 1, *B, center*; after inhalation). In contrast, the number of RFP^+ CD4 T cells from nonimmunized mice did not increase in the lung (Fig 1, *B and C*). These results indicate that CD4 T-cell migration into the lung after ovalbumin inhalation is ovalbumin priming–dependent. When we used the opposite color-coded immunization pattern, only the ovalbumin-primed RFP^+ CD4 T cells accumulated in the lung, not the nonprimed GFP^+ CD4 T cells (see this article's Fig E1, *A and B*, in the Online Repository at www.jacionline.org). These results indicate that the

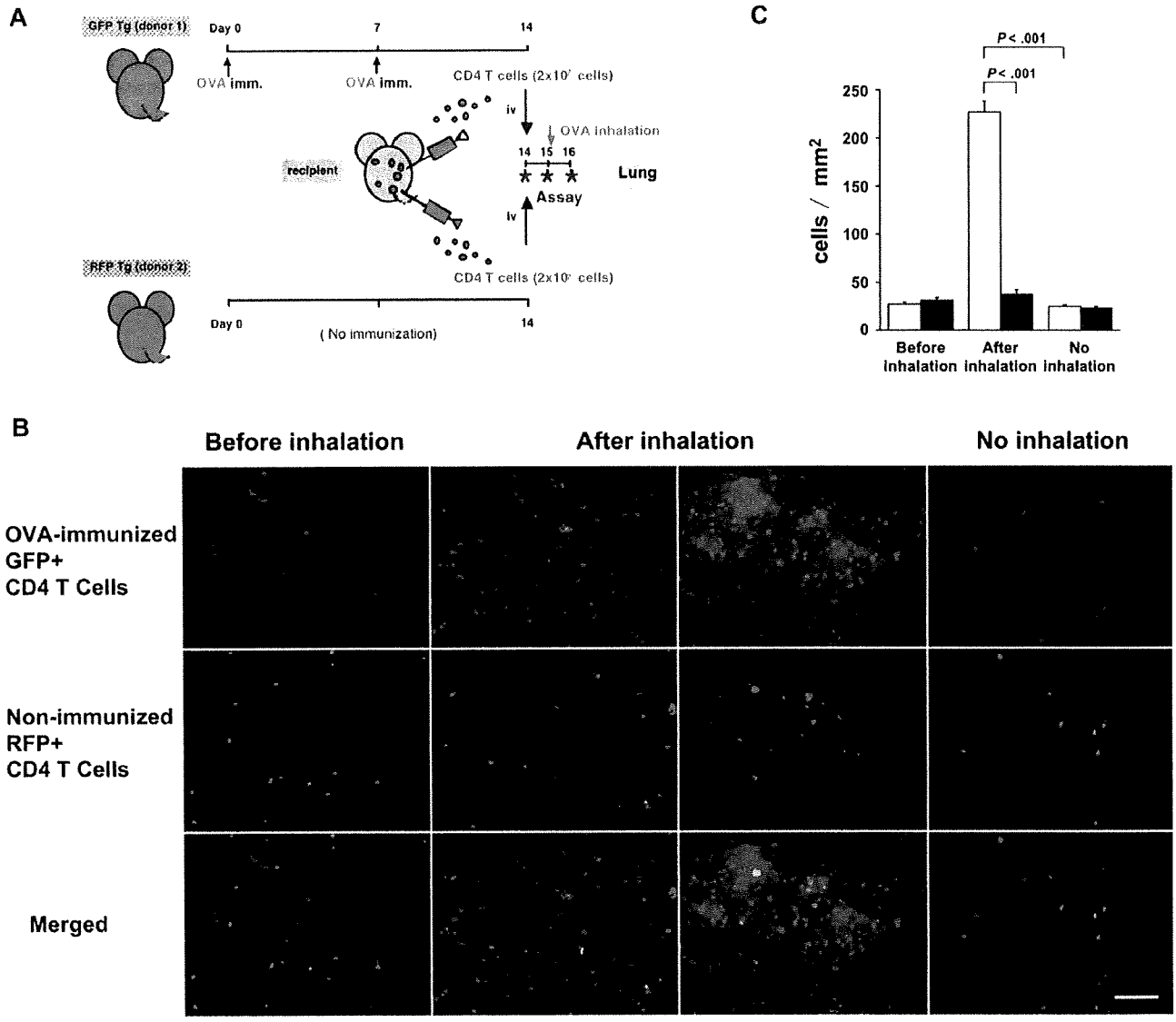

FIG 1. Color-coded fluorescence imaging of ovalbumin *(OVA)*-primed CD4 T-cell accumulation in the lung in the OVA-induced acute asthma model. **A,** A schematic overview of the study protocol for the induction of asthma. GFP Tg mice were sensitized with OVA on days 0 and 7. Splenic CD4 T cells from OVA-sensitized GFP Tg and nonsensitized RFP Tg mice were purified and injected into normal C57BL/6 mice on day 14. The recipient mice were exposed to airway challenge with aerosolized OVA on day 15. **B,** Color-coded images of GFP^+ and RFP^+ CD4 T cells. GFP^+ and RFP^+ CD4 T cells in the excised lung were monitored before OVA inhalation on day 15 and 24 hours after OVA inhalation on day 16 by using the OV100 Small Animal Mouse Imaging System. *Bar,* 100 μm. **C,** Summary of the accumulation of fluorescent cells. Data are from 15 fields from 3 mice with SD. *Open bar,* GFP; *closed bar,* RFP. $*P < .001$ by the Student's *t* test.

difference in accumulation is not fluorescent protein–dependent. Furthermore, we examined the migration of naive antigen-specific CD4 T cells in the lung. Ovalbumin-specific CD4 T cells were prepared from nonimmunized mice derived by crossing GFP Tg mice with OT II Tg mice, which have ovalbumin-specific, MHC class II–restricted αβ T-cell receptors.[19] Most of the CD4 T cells in the OT II Tg mice are ovalbumin-specific. Ovalbumin-specific CD4 T cells were transferred intravenously into normal C57BL/6 mice 24 hours before airway challenge with aerosolized ovalbumin. Twenty-four hrs after ovalbumin inhalation, GFP^+ cells in the excised lungs were monitored by fluorescence imaging. The number of GFP^+ OT II Tg–CD4 T cells did not increase in the lung (see this article's Fig E2 in the Online Repository at www.jacionline.org). These results indicate that even antigen-specific CD4 T cells do not accumulate in the lung after allergen challenge if the cells are not primed.

Imaging of ovalbumin-specific OT II–T_H2 cell accumulation into the lung and the generation of GFP^+ T_H2 cell foci in a mouse model of asthma

To investigate the dynamics of accumulating antigen-specific effector T cells in the lung of living mice in a mouse model of asthma, ovalbumin-specific T_H2 cells (OT II–Tg–T_H2) were

prepared *in vitro* from naive CD4 T cells obtained from GFP^+ OT II Tg mice. Ovalbumin-specific OT II–Tg–T_H2 cells expressing GFP were transferred intravenously into normal C57BL/6 mice. Immediately after cell transfer, numerous transferred cells temporally and nonspecifically accumulated in the lung capillaries (data not shown). Twenty-four hours after cell transfer, the recipient mice were exposed to allergen challenge with aerosolized ovalbumin. GFP^+ OT II–T_H2 cells were imaged under fluorescence microscopy at various time points as long as 24 hours after ovalbumin inhalation by excising the lung (Fig 2, *A*). The accumulation of GFP^+ OT II–T_H2 cells in the lung was detected beginning 6 hours after allergen inhalation. The maximum number of OT II–T_H2 cells accumulated between 18 and 24 hours. GFP^+ OT II–T_H2 cells formed small foci 6 hours after ovalbumin inhalation (Fig 2, *A*). The number of foci increased, and their mean size also increased at 12 hours. The number of foci in the lungs further increased (18 hours). Nonfocal GFP^+ cells also greatly increased in the lung. At 18 hours or later, the border of the foci became diffuse, and many foci appeared to be fused. For color-coded imaging of the migration of nonprimed CD4 T cells around the OT II–T_H2-cell foci, GFP^+ OT II–T_H2 cells and splenic CD4 T cells from nonsensitized RFP Tg mice were purified and intravenously transferred together into normal C57BL/6 mice 24 hours before airway challenge with aerosolized ovalbumin. Twenty-four hours after ovalbumin inhalation, GFP^+ and RFP^+ cells in the excised lungs were monitored by fluorescence imaging. The number of RFP^+ CD4 T cells from nonimmunized mice did not increase around the OT II–T_H2 cell foci (see this article's Fig E3 in the Online Repository at www.jacionline.org). These results indicate that unprimed CD4 T cells do not accumulate in the foci formed by antigen-specific T_H2 cells. We have performed time course experiments. Most antigen-specific T_H2 cells accumulated in the lung within 24 hours after antigen inhalation. The accumulated cells that formed foci remained as long as 72 hours after antigen inhalation (data not shown).

Real-time cellular dynamics of T_H2-cell accumulation in the lung of living mice in a mouse model of asthma

Real-time cellular dynamics of antigen-specific T_H2-cell accumulation into the lung was then imaged in living mice at the cellular level by using scanning laser fluorescence microscopy. To image this process, antigen-specific T_H2 cells generated *in vitro* from naive CD4 T cells of GFP^+ OT II Tg mice were transferred intravenously into normal C57BL/6 mice. The recipient mice were administered ovalbumin by inhalation. They were then anesthetized and tracheostomized, and the lung was exposed microsurgically at various time points after ovalbumin inhalation. First, to assess any changes in blood flow rates in the clamped right lung and ventilated left lung, fluorescent microspheres were infused before and after clamping and ventilation. The lungs were then monitored by fluorescence microscopy (see this article's Fig E4 in the Online Repository at www.jacionline.org). Thirty minutes after clamping and ventilation, blood flow rates in both lungs were comparable. The relative blood flow was still kept at more than 80% of that before clamping and ventilation. Thus, the relative blood flow rates in the clamped lung appeared not to be changed in this experimental system.

The clamped right lungs were then imaged with the IV100 scanning laser microscope. Before ovalbumin inhalation, no foci were observed in the lung (Fig 2, *B*; Table I; see this article's Video E1 in the Online Repository at www.jacionline.org). The rate of rolling GFP^+ T_H2 cells in the field was 14.7 + 1.5 cells/mm^2/30 min. Some of the rolling cells attached and accumulated in the field (7.0 + 1.5 cells/mm^2/30 min), and a similar amount of the T_H2 cells egressed from the field (7.0 + 1.0 cells/mm^2/30 min). These results suggest that the allergen-specific effector T cells were rolling in the lung vessels, and some were migrating into and accumulating in the lung, whereas some were migrating out of the lung. At time 0, the ratio of cells that accumulated and egressed from the field was equivalent, and the total cell number in the lung appeared to be maintained at a constant level. Only 10% of the T_H2 cells in the lung were crawling in this stable state (see this article's Video E2 in the Online Repository at www.jacionline.org). Six hours after ovalbumin inhalation, small foci were observed (Fig 2, *B, red asterisks*). By 6 hours, the number of rolling T_H2 cells greatly increased compared with the stable state (33.3 + 3.1 vs 14.7+1.5 cells/mm^2/30 min; Table I). GFP^+ T_H2-cell accumulation in the lung also increased (15.3 + 1.5 cells/mm^2/30 min; Table I; see this article's Video E3 in the Online Repository at www.jacionline.org). The degree of GFP^+ T_H2-cell egress from the field was similar to that observed in the stable state. By 6 hours, the ratio of crawling cells was observed to increase (30.5% from 10.0%). These observations suggest that the allergen-induced migration and accumulation of T_H2 cells into the lung began to be upregulated by 6 hours after ovalbumin inhalation. The formation of foci was also observed approximately 6 hours after ovalbumin inhalation. Twelve hours after ovalbumin inhalation, the foci became larger, and the number of T_H2 cells rolling in the field further increased (44.7 + 4.5 cells/mm^2/30 min; Table I; see this article's Video E4 in the Online Repository at www.jacionline.org). T_H2-cell accumulation in the lung also further increased (24.3 + 2.5 cells/mm^2/30 min). However, the degree of T_H2-cell egress from the field did not obviously change compared with that observed in the stable state (8.3 + 1.6 vs 7.0 + 1.0). At 12 hours after ovalbumin inhalation, 90% of the T_H2 cells accumulating in the field were crawling (see this article's Video E5 in the Online Repository at www.jacionline.org). Thus, allergen-induced migration and accumulation of T_H2 cells into the lung appeared to be highly upregulated at approximately 12 hours after ovalbumin inhalation. At 21 hours after ovalbumin inhalation, nonfocal T_H2 cells greatly increased (868.7 + 296.5 cells/mm^2/30 min at 21 hours). More than 95% of the accumulating cells were crawling at this time point. However, at 21 hours, T_H2 cells rolling into the field were apparently reduced (2.7 + 0.6 cells/mm^2/30 min; Table I; see this article's Video E6 in the Online Repository at www.jacionline.org). Therefore, the allergen-induced migration and accumulation of T_H2 cells into the lung reached maximum levels by 21 hours after ovalbumin inhalation. Between 6 and 12 hours after ovalbumin inhalation, the migrating T_H2 cells predominantly formed foci. Later, at 12 to 21 hours after ovalbumin inhalation, the T_H2 cells were observed to accumulate throughout the lung rather than form foci.

Effect of dexamethasone on the accumulation of ovalbumin-primed CD4 T cells in the lung in a mouse model of asthma

The color-coded imaging system was then used to determine the effect of dexamethasone, a potent drug that attenuates

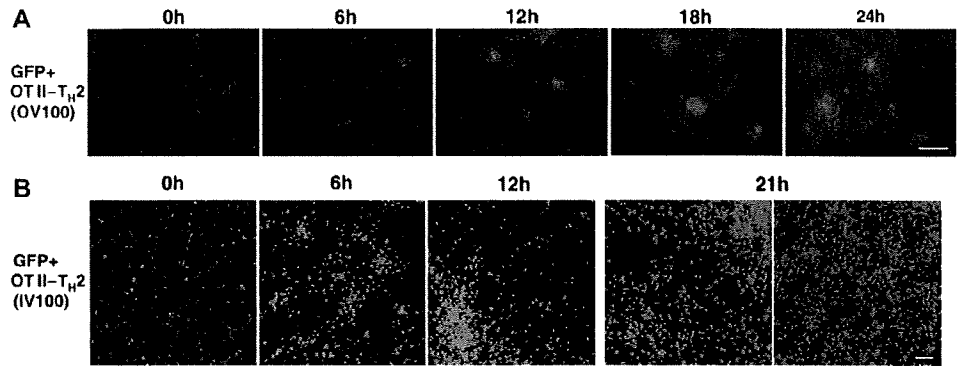

FIG 2. Imaging of ovalbumin-specific OT II–T_H2-cell accumulation in the lung and the generation of GFP^+ T_H2-cell foci after ovalbumin inhalation. GFP^+ OT II–T_H2 cells, differentiated *in vitro* from naive CD4 T cells from GFP^+ OT II Tg mice, were intravenously transferred into C57BL/6 mice. Two days later, the recipient mice were administered ovalbumin by inhalation. The mice were subjected to imaging at indicated time points after ovalbumin inhalation. GFP^+ T_H2 cells were imaged by using the OV100 Small Animal Imaging System **(A)** or the IV100 scanning laser imaging system **(B)**. *Red asterisks* indicate the site of focus formation. *Bar*, 300 μm *(A)* and 100 μm *(B)*. The results are representative of 5 *(A)* and 3 *(B)* experiments.

TABLE I. Summary of nonfocal OT II–T_H2 cell accumulation in the lung after ovalbumin inhalation

After ovalbumin inhalation	0 h	6 h	12 h	21 h
Cell number in nonfocal area (cells/mm^2)	57.7 ± 4.5	134.3 ± 16.9	226.0 ± 25.1	868.7 ± 296.5
Cells rolling in the blood vessel (cells/mm^2/30 min)	14.7 ± 1.5	33.3 ± 3.1	44.7 ± 4.5	2.7 ± 0.6
Cells accumulated in the field (cells/mm^2/30 min)	7.0 ± 1.5	15.3 ± 1.5	24.3 ± 2.5	1.3 ± 0.6
Cells egressed from the field (cells/mm^2/30 min)	7.0 ± 1.0	8.0 ± 1.5	8.3 ± 1.6	0.7 ± 0.6
Cells crawling in the field (%)	10.0	30.5	90.0	96.0

The data are presented as the mean cell number + SD from 3 independent experiments unless otherwise indicated.

allergic reactions, on the accumulation of allergen-primed CD4 T cells in the lung. Dexamethasone (0.4, 1, or 4 mg/kg) was administered intraperitoneally 1 hour before ovalbumin inhalation. GFP^+ CD4 T cells were monitored by fluorescence imaging 24 hours after ovalbumin inhalation. A marked dexamethasone dose-dependent decrease in the number of infiltrated CD4 T cells was observed in the excised lung (Fig 3, *A and B*). These results suggest that the efficacy of dexamethasone in inhibiting the development of ovalbumin-induced airway inflammation was, at least in part, a result of the inhibition of CD4 T-cell accumulation into the lung. Dexamethasone was then administered intraperitoneally after ovalbumin inhalation (on day 16), and GFP^+ CD4 T cells were monitored by fluorescence imaging 1 day later. The extent of infiltration of GFP^+ CD4 T cells was again observed to decrease significantly (Fig 3, *C and D*). These results indicate that the infiltration of CD4 T cells was reduced if dexamethasone was administered even after the onset of airway inflammation.

Contribution of adhesion molecules to the generation of T_H2-cell foci in the lung in a mouse model of asthma

We next assessed the contribution of adhesion molecules to the generation of T_H2-cell foci in the lung in a mouse model of asthma. The blockage of ICAM-1 and VCAM-1 by antibodies to these molecules is known to inhibit airway inflammation.[14] To test the role of ICAM-1 and VCAM-1 in our model, GFP^+ OT II–T_H2 cells were transferred intravenously into normal C57BL/6 mice. One day before ovalbumin inhalation, mice were injected intraperitoneally with 200 μg anti–ICAM-1 (YN1/1.7.4) or anti–VCAM-1 (429) mAbs. One day after ovalbumin inhalation, transferred ovalbumin-specific GFP^+ T_H2 cells were monitored by using fluorescence imaging. The generation of GFP^+ T_H2-cell foci in the lung was substantially inhibited by treatment with anti–ICAM-1 and anti–VCAM-1 mAbs (Fig 3, *E and F*). Our model demonstrates that ICAM-1 and VCAM-1 play an essential role in focus formation by the control of T_H2-cell migration in the lung. Thus, T_H2 focus formation appears to be critical in the development of allergic airway inflammation in this animal model.

Eosinophilic infiltration and GFP^+ T_H2-cell infiltration into the lung in a mouse model of asthma

Previous studies in animal models suggest a T_H2 paradigm for allergic diseases, with an increased activation of T_H2 cells that produce T_H2 cytokines, thereby resulting in the recruitment and activation of eosinophils. Marked eosinophilic infiltration is characteristic 2 or 3 days after allergen challenge in animal models of allergic airway inflammation.[7,9,10] The foci formed by T_H2 cells observed in the current study and accumulation of eosinophils may be coincidental because our results showed